

# Improving Action Smoothness of a Cascaded Online Learning Flight Control System

Yifei Li, Erik-Jan van Kampen

## Abstract

Model-free reinforcement learning has demonstrated the capability to adjust control laws using data-constructed policy gradients. Its application to online flight control commonly adopts a cascaded control architecture, which enables efficient policy learning for angle-of-attack tracking using control-surface deflections. However, the tracking performance and system stability are degraded by oscillatory actions. To address this issue, we incorporate policy regularization for temporal action smoothness and a low-pass filter to attenuate both the amplitude and oscillatory frequency of actions. The Fast Fourier Transform (FFT) algorithm is used to analyze action smoothness in the frequency-domain representation. Flight control simulations demonstrate the effectiveness of the two proposed techniques.

## Index Terms

reinforcement learning, symmetry, data augmentation, approximate value iteration, flight control.

## I. INTRODUCTION

Model-free reinforcement learning (RL) has been applied to flight control law optimization without using a system model for state prediction. The policy gradient is constructed using measured data. This approach significantly reduces the design effort required to model the complex dynamics of aerial vehicles. Implementing model-free RL for nonlinear control using ADP does not require learning a full system model, since only the first-order derivatives of the system dynamics are needed to construct the policy gradients. This observation motivates the use of a simpler model with fewer parameters than an artificial neural network, while still capturing the required first-order derivatives, such as an *incremental model*, thereby simplifying training. The incremental model is a local linear approximation of a nonlinear system derived using a Taylor expansion. Its combination with linear Recursive Least Squares (RLS) identification applied to ADP has led to the development of incremental model-based ADP (IADP) methods, enabling computationally efficient online policy learning. Compared with Action Dependent Heuristic Dynamic Programming (ADHDP), which implicitly approximates the control effectiveness within a state-action ( $Q$ ) function, the RLS algorithm identifies the control effectiveness more quickly and accurately. This leads to a more reliable construction of the policy gradient, as demonstrated in simple cases. For example, the Incremental model-based Heuristic Dynamic Programming (IHDP) requires only the signs of control effectiveness matrix  $G$  to construct policy gradients. Other variants of IADP include incremental model-based dual heuristic programming (IDHP), and incremental model-based global dual heuristic programming (IGDHP). These methods have been applied to online policy optimization for tracking control of pitch rate, angle of attack (AOA), and altitude for the Flying-V, the Cessna Citation business jet, and the F-16 model.

For online learning-based AOA tracking control, a *cascaded* control structure is typically used to separately regulate angle-of-attack tracking and pitch-rate tracking in the outer-loop and the inner-loop control systems. This *hierarchical* control strategy explicitly incorporates pitch-rate constraints to prevent overly aggressive rate responses. When using a monolithic structure, the pitch rate can also be constrained through penalization in the reward design, but unguided rate control degrades overall performance. In addition, the rate control is highly sensitive to the weighting of the pitch-rate loss term. These discussions underscore the importance of a well-designed pitch-rate reference for ensuring reliable control performance. An illustrative example is backstepping, where a stabilizing pitch-rate reference policy is derived from a nominal model to ensure the convergence of tracking errors, and adaptive laws are implemented to handle model uncertainties.

However, designing a stabilizing pitch-rate reference is challenging in model-free IADP methods, which rely solely on measured data for reference design. The resulting imprecise pitch-rate reference makes it difficult to ensure system stability. Another challenge is that the statistical performance of tracking errors near zero is degraded by time-varying nonlinear dynamics and time-varying reference signals, resulting in frequently switching tracking errors. These errors, in turn, generate switching pitch-rate references through the outer-loop actor, further perturbing the control surface deflections in the inner-loop control system. (a phenomenon observed in switching control laws). This is a more serious issue than in learning-based control of linear time-invariant (LTI) systems.

Yifei Li was with the Section Control and Simulation, Faculty of Aerospace Engineering, Delft University of Technology, Delft, 2629 HS, the Netherlands, e-mail: y.li-34@tudelft.nl.

Erik-Jan van Kampen was with the Section Control and Simulation, Faculty of Aerospace Engineering, Delft University of Technology, Delft, 2629 HS, the Netherlands, e-mail: e.vankampen@tudelft.nl.

Manuscript received Month Day, Year; revised Month Day, Year.

A second factor contributing to state and action oscillations is actor saturation. A saturated actor responds to tracking errors with actions near their maximum or minimum limits, exhibiting almost bang–bang control behavior. Furthermore, because the saturated activation function produces vanishing policy gradients, the actor weights become nearly fixed and difficult to adjust. To mitigate this problem, a discounted learning rate has been used to slow down actor updates over time, reducing the likelihood of entering the saturation region. However, the choice of the discounted learning rate is empirical and sensitive, and it does not prevent actor saturation as learning progresses. Another potential solution is to terminate policy learning by fixing the actor weights once the required control performance is achieved, either by specifying a termination time or setting a tracking error threshold, a strategy that has not yet been studied.

This paper addresses state oscillations by first introducing a temporal smoothness loss into the model-free IHDP framework. While this approach has been studied in offline RL algorithms, it has not yet been explored in online learning with limited samples. Second, unresolved high-frequency actions are attenuated using a low-pass filter, whose effectiveness has been demonstrated in command-filtered backstepping.

The main contributions are summarized as:

- Temporal action smoothness is incorporated into online policy learning and formulated within a multi-objective optimization framework.
- A low-pass filter is applied to smooth the pitch-rate reference to further improve action smoothness.
- The termination and restart conditions are designed based on the accumulated tracking errors, enabling the RL agents to autonomously decide when to stop or restart learning.

The remainder of this paper is structured as follows. Section II presents the aerial vehicle model and its formulation as a single-input–single-output system. Section III formulates optimization-based tracking control design. Section IV presents the cascaded online RL framework, followed by introducing two action-smoothing techniques in Section IX. Section X presents flight control simulations with action-smoothing techniques. Section XI concludes this paper.

#### A. Related Work

- 1) *Data-driven policy optimization:*
- 2) *IADP for flight control:*

## II. MODEL

This section introduces a longitudinal model of aerial vehicles, which is then expressed in state-space form for convenient flight-control design.

#### A. Aerial Vehicle Model

The dynamical model of aerial vehicles is given as [32]

$$\begin{aligned}\dot{\alpha} &= \left( \frac{fgQS}{WV} \right) \cos(\alpha) [\phi_z(\alpha) + b_z \delta] + q \\ \dot{q} &= \left( \frac{fQSa}{I_{yy}} \right) [\phi_m(\alpha) + b_m \delta]\end{aligned}\tag{1}$$

where  $\alpha$  is the angle of attack,  $q$  is the pitch rate,  $\delta$  is the control surface deflection. The aerodynamic coefficients are approximately computed by  $b_z = -0.034$ ,  $b_m = -0.206$ , and

$$\begin{aligned}\phi_z(\alpha) &= 0.000103\alpha^3 - 0.00945\alpha|\alpha| - 0.170\alpha \\ \phi_m(\alpha) &= 0.000215\alpha^3 - 0.0195\alpha|\alpha| - 0.051\alpha\end{aligned}\tag{2}$$

These approximations of  $b_z$ ,  $b_m$ ,  $\phi_z(\alpha)$ ,  $\phi_m(\alpha)$  hold for  $\alpha$  in the range of  $\pm 20$  degrees. The physical coefficients are provided in Table I. In addition, the actuator dynamics are considered as a first order model with the time constant 0.005s. The rate limit is 600 deg/s, and a control surface deflection limit is  $\pm 20$  degrees.

#### B. Formulation of a Single-input-single-output system

The differential equations 1 can be reformulated as

$$\begin{aligned}\dot{x}_1 &= f_1(x_1) + x_2 + d_1(x_1, u) \\ \dot{x}_2 &= f_2(x_1) + g_2 u\end{aligned}\tag{3}$$

TABLE I: Physical parameters (adapted from [32])

Notations	Definition	Value
$g$	acceleration of gravity	9.815 m/s <sup>2</sup>
$W$	weight	204.3 kg
$V$	speed	947.715 m/s
$I_{yy}$	pitch moment of inertia	247.438 kg·m <sup>2</sup>
$f$	radians to degrees	180/π
$Q$	dynamic pressure	29969.861 kg/m <sup>2</sup>
$S$	reference area	0.041 m <sup>2</sup>
$d$	reference diameter	0.229 m

where  $[x_1, x_2]^T = [\alpha, q]^T$ ,  $u = \delta$  are state and control input. The nonlinear functions are defined as

$$\begin{aligned} f_1(x_1) &= \left( \frac{fgQS}{WV} \right) \cos(\alpha)\phi_z(\alpha), & d_1(x_1, u) &= \left( \frac{fgQS}{WV} \right) \cos(\alpha)b_z \\ f_2(x_1) &= \left( \frac{fQScd}{I_{yy}} \right) \phi_m(\alpha), & g_2(x_1, \delta) &= \left( \frac{fQScd}{I_{yy}} \right) b_m \end{aligned} \quad (4)$$

The model 3 is a single-input-single-output (SISO) system, as it has a single input that controls the state  $x_2$  and subsequently influence the state  $x_1$  through near-integrator dynamics, which exhibits dynamical oscillations when rate control is loose. The additional aerodynamic dynamics  $f_1(\cdot)$  also disturb the angle-of-attack tracking error and the resulting control actions.

### III. OPTIMIZATION-BASED TRACKING CONTROL DESIGN

This section firstly derives the tracking errors dynamics. Then the optimization-based tracking control methods are formulated to design control laws for the outer-loop and the inner-loop subsystems.

#### A. Tracking errors dynamics

Define the tracking errors as  $e_1 = \alpha - \alpha_{\text{ref}}$ ,  $e_2 = q - q_{\text{ref}}$ , one has

$$\begin{aligned} \dot{e}_1 &= \dot{\alpha} - \dot{\alpha}_{\text{ref}} \\ &= f_1(x_1) + x_2 + d_1 - \dot{\alpha}_{\text{ref}} \\ &= f_1(x_1) + e_2 + q_{\text{ref}} + d_1 - \dot{\alpha}_{\text{ref}} \end{aligned} \quad (5)$$

$$\begin{aligned} \dot{e}_2 &= \dot{q} - \dot{q}_{\text{ref}} \\ &= f_2(x_1) + g_2 u - \dot{q}_{\text{ref}} \end{aligned} \quad (6)$$

where  $\alpha_{\text{ref}}$ ,  $q_{\text{ref}}$  are the angle-of-attack reference and the pitch rate reference.

The virtual control defined as  $q_{\text{ref}}(e_1, \alpha, \delta)$  is associated with  $e_1, \alpha, \delta$ , aiming to provide error-feedback control for stabilizing  $e_1$  and from the intuitive point of view, compensate for the dynamics associated with  $\alpha$  and  $\delta$  in  $e_1$ -subsystem. In backstepping this nominal model is used to design the virtual control and its adaptive variants to ensure asymptotic convergence of the tracking errors under model uncertainties. In model-free RL settings, the design of  $q_{\text{ref}}(e_\alpha, \alpha, \delta)$  with guaranteed performance is infeasible as the dynamics are unknown. It is usually parameterized using a neural network and trained with samples. The same analysis applies to the design of  $u$  in  $e_2$ -subsystem. The control surface deflection  $\delta = u(e_2, q, \alpha)$  is a function of  $e_2, q$  and  $\alpha$ , in order to stabilize  $e_2$  and compensate for the dynamics associated with  $q, \alpha$ .

#### B. Optimization-based tracking control

Infinite-horizon optimal tracking control problems are formulated for angle-of-attack tracking and pitch rate tracking.

For the  $e_1$ -subsystem, a continuous scalar state-value function starting from  $t$  is denoted as  $V_1(t) : \mathbb{R}^3 \rightarrow \mathbb{R}_+$  and defined by

$$V_1(t) = \int_t^\infty c_1(\tau) d\tau \quad (7)$$

where  $c_1(t) = e_1^2(t) + a q_{\text{ref}}^2(t)$  is the one-step cost,  $a \in \mathbb{R}_+$  trades off between tracking error and control effort.  $\mathbb{R}_+$  denotes the set of non-negative real numbers. The optimal control law is defined as

$$q_{\text{ref}}^*(t) \in \arg \min_{q_{\text{ref}}} V_1(t) \quad (8)$$

For the  $e_2$ -subsystem, a state-value function starting from  $t$  is denoted as  $V_2(t) : \mathbb{R}^2 \rightarrow \mathbb{R}_+$  and defined by

$$V_2(t) = \int_t^\infty c_2(\tau) d\tau \quad (9)$$

where  $c_2(t) = e_2^2(t) + bu^2(t)$  is the one-step cost.  $b \in \mathbb{R}_+$  trades off between tracking error and control effort. The optimal control law is defined as

$$\delta^*(t) \in \arg \min_{\delta} V_2(t) \quad (10)$$

#### IV. MODEL-FREE REINFORCEMENT LEARNING IMPLEMENTATION

This section introduces an online reinforcement learning framework for angle-of-attack tracking control. A cascaded control structure is employed for separate control of angle-of-attack tracking and pitch rate tracking [20], [22]. The learning process is a sample-based implementation of the optimization-based tracking control design in Section III. The learning algorithm uses Incremental model-based heuristic dynamic programming (IHDP).

##### A. Networked control laws

The sub-control laws are parameterized using two neural networks:

###### Outer-loop control law

$$q_{\text{ref}}(e_1, \alpha, \delta) = W_1(e_1, \alpha, \delta) \quad (11)$$

###### Inner-loop control law

$$\delta(e_2, q, \alpha) = W_2(e_2, q, \alpha) \quad (12)$$

###### Nested control law

$$\delta(e_2, q, \alpha) = W_2(q - \underbrace{W_1(e_1, \alpha, \delta)}_{\text{outer-loop actor}}, q, \alpha) \quad (13)$$

inner-loop actor

where  $W_1(\cdot; w^{A_1}), W_2(\cdot; w^{A_2})$  are neural networks with trainable parameter sets  $w^{A_1}, w^{A_2}$ . The cascaded structure is illustrated in Figure 1, along with a comparison to the monolithic actor.

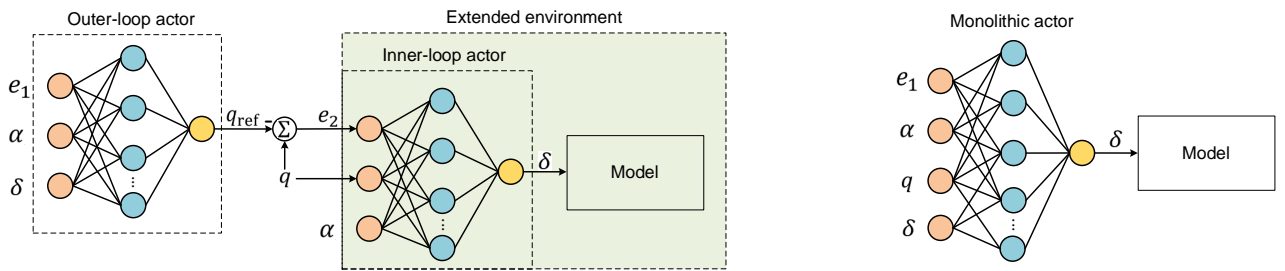


Fig. 1: Cascaded actor versus monolithic actor. The former uses an outer-loop actor to generate a pitch-rate reference, which is then passed to an inner-loop actor that produces the control-surface deflection, providing an explicit mechanism for learning and tracking the pitch-rate reference. The latter is a fully connected multilayer perceptron (MLP) that approximates an end-to-end tracking policy. The pitch-rate reference is not explicitly represented by the monolithic actor. This end-to-end structure is commonly used for the stabilization of inverted pendulum and Van der Pol's oscillator, without additional angular dynamics.

### B. Incremental model-based heuristic dynamic programming

IHDP can be employed to perform online model-free policy optimization [24]. The incremental model is a local linear approximation of a nonlinear system, which provides a direct representation of the first-order partial derivatives of the system dynamics. These derivatives are used to construct the gradient from the next-step state to the action, as a component of the policy gradient. This approach reduces the computational load for training a system model compared with a neural-network-based model in HDP. This advantage becomes more pronounced in model-free implementations of HDP and IHDP, where the model does not need to be accurate to ensure reliable state prediction and subsequent policy learning.

The incremental model of  $q$ -dynamics is developed as

$$\Delta q_{t+1} = F_{t-1} \Delta q_t + G_{t-1} \Delta \delta_t \quad (14)$$

where the subscript  $t$  denotes the discrete-time index. The state increments are defined as  $\Delta q_{t+1} = q_{t+1} - q_t$ ,  $\Delta q_t = q_t - q_{t-1}$ , the control increment is defined as  $\Delta \delta_t = \delta_t - \delta_{t-1}$ . The first-order partial derivatives are  $F_{t-1} = \frac{\partial f_2}{\partial \alpha} |_{\alpha_{t-1}, \delta_{t-1}, q_{t-1}}$ ,  $G_{t-1} = \frac{\partial g_2 u}{\partial \delta_t} |_{\alpha_{t-1}, \delta_{t-1}, q_{t-1}}$ . The derivation is seen in Appendix XI-A. In practice, the model is identified using linear Recursive Least Squares algorithm (Appendix XI-B).

**Remark 1.** The incremental model of the  $\alpha$ -dynamics is not required during the training of the outer-loop actor, even though its task is to control angle-of-attack. This control effectiveness from  $q$  to  $\alpha$  is implicitly captured in the estimated value function  $\hat{V}_2(\cdot)$  by taking  $q$  as an input.

## V. INCREMENTAL MODEL-BASED HEURISTIC DYNAMIC PROGRAMMING

### A. Problem formulation

Consider a discrete-time nonlinear dynamical system as

$$x(t+1) = f(x(t), u(t)), \quad (15)$$

where  $x \in \mathbb{R}^m$  is the state vector and  $u \in \mathbb{R}^n$  is the control vector.

The cost-to-go function is expressed as

$$J(x(t)) = \sum_{i=t}^{\infty} \alpha^{i-t} r(x(i), u(i)), \quad (16)$$

where  $\alpha \in (0, 1]$  is the discount factor,  $r(x(t), u(t))$  is the reward function. We require  $r(t) = r(x(t), u(t))$  to be a bounded semidefinite function of the state and control so that the cost function is well defined. One can obtain from (16) that  $0 = J(t) - r(t) - \alpha J(t+1)$ , where  $J(t) = J(x(t))$ .

### B. Critic network

The critic network is a one-hidden-layer multilayer perceptron (MLP) that takes the input as  $y(t) = (x_1(t), \dots, x_m(t))^T$  and the output as  $\hat{J}(t)$  to approximate  $J(t)$ . The number of nodes in hidden layer is  $N_{h_c}$ . The weight between input node  $i$  and hidden node  $j$  is  $\hat{w}_{c,ji}^{(1)}(t)$ . The weight between hidden node  $j$  and output node is  $\hat{w}_{c,j}^{(2)}(t)$ .

The input to hidden node  $j$  is:

$$\sigma_{c,j}(t) = \sum_{i=1}^m \hat{w}_{c,ji}^{(1)}(t) x_i(t) \quad (17)$$

The output of hidden node  $j$  is

$$\phi_{c,j}(t) = \tanh(\sigma_{c,j}(t)) \quad (18)$$

where  $\tanh(\cdot)$  is the nonlinear activation function.

The output of the critic is

$$\hat{J}(t) = \sum_{j=1}^{N_{h_c}} \hat{w}_{c,j}^{(2)}(t) \phi_{c,j}(t), \quad (19)$$

### C. Actor network

The actor network is a one-hidden-layer multilayer perceptron (MLP) that takes the input as the state  $x(t) = (x_1(t), \dots, x_m(t))^T$ , and the output as the action. The number of nodes in hidden layer is  $N_{h_a}$ . The weight between input node  $i$  and hidden node  $j$  is  $\hat{w}_{a,ji}^{(1)}(t)$ . The weight between hidden node  $j$  and output node  $k$  is  $\hat{w}_{a,kj}^{(2)}(t)$ .

The input to hidden node  $j$  is

$$\sigma_{a,j}(t) = \sum_{i=1}^m \hat{w}_{a,ji}^{(1)}(t) x_i(t). \quad (20)$$

The output of hidden node  $j$  is:

$$\phi_{a,j}(t) = \tanh(\sigma_{a,j}(t)) \quad (21)$$

The output of the output node  $k$  is

$$u_k(t) = \sum_{j=1}^{N_{h_a}} \hat{w}_{a,kj}^{(2)}(t) \phi_{a,j}(t) \quad (22)$$

## VI. GRADIENT-DESCENT ALGORITHM

### A. Update of the critic network

The critic network is trained to minimize the objective function  $E_c(t) = \frac{1}{2}e_c^2(t)$ , where  $e_c(t) = \hat{J}(t) - r(t) - \alpha\hat{J}(t+1)$  is the Bellman error. This definition in ADHDP [Ref] follows a backforward style due to the convenience of policy improvement using state-action value function.

The weights between the input layer and the hidden layer are updated by

$$\hat{w}_c^{(1)}(t+1) = \hat{w}_c^{(1)}(t) + \Delta\hat{w}_c^{(1)}(t) \quad (23)$$

where  $\hat{w}_c^{(1)} \in \mathbb{R}^{N_{h_c} \times m}$ .

According to the gradient descent:

$$\Delta\hat{w}_{c,ji}^{(1)}(t) = l_c \left[ -\frac{\partial E_c(t)}{\partial \hat{w}_{c,ji}^{(1)}(t)} \right] \quad (24)$$

which follows from the chain rule

$$\begin{aligned} \frac{\partial E_c(t)}{\partial \hat{w}_{c,ji}^{(1)}(t)} &= \frac{\partial E_c(t)}{\partial e_c(t)} \frac{\partial e_c(t)}{\partial \hat{J}(t)} \frac{\partial \hat{J}(t)}{\partial \phi_{c,j}(t)} \frac{\partial \phi_{c,j}(t)}{\partial \sigma_{c,j}(t)} \frac{\partial \sigma_{c,j}(t)}{\partial \hat{w}_{c,ji}^{(1)}(t)} \\ &= e_c(t) \hat{w}_{c,j}^{(2)}(t) \phi'_{c,j}(t) y_i(t) \end{aligned} \quad (25)$$

The weights between the hidden layer and the output layer are updated by

$$\hat{w}_c^{(2)}(t+1) = \hat{w}_c^{(2)}(t) + \Delta\hat{w}_c^{(2)}(t) \quad (26)$$

where  $\hat{w}_c^{(2)} \in \mathbb{R}^{1 \times N_{h_c}}$ .

According to the gradient descent:

$$\Delta\hat{w}_{c,j}^{(2)}(t) = l_c \left[ -\frac{\partial E_c(t)}{\partial \hat{w}_{c,j}^{(2)}(t)} \right] \quad (27)$$

which follows from the chain rule

$$\frac{\partial E_c(t)}{\partial \hat{w}_{c,j}^{(2)}(t)} = \frac{\partial E_c(t)}{\partial e_c(t)} \frac{\partial e_c(t)}{\partial \hat{J}(t)} \frac{\partial \hat{J}(t)}{\partial \phi_{c,j}(t)} = e_c(t) \phi_{c,j}(t) \quad (28)$$

### B. Update of the actor network

The actor network is trained according to  $\hat{J}(t)$ , which is reconstructed from the Bellman equation as  $\hat{J}(t) = r(t) + \alpha\hat{J}(t+1)$ , rather than a state-action value function  $\hat{J}(x(t), u(t))$  as in ADHDP [Ref]. (In this paper, we use an importance-weighted training approach). (Let  $U_c$  denote the desired ultimate objective function. The quadratic error measure to be minimized is  $E_a(t) = \frac{1}{2}e_a^2(t)$ ,  $e_a(t) = r(t) + \alpha\hat{J}(t+1) - U_c$ . In reinforcement learning, success corresponds to an objective that is zero at each time step. For simplicity of derivation, we assume  $U_c = 0$ , i.e.  $e_a(t) = r(t) + \alpha\hat{J}(t+1)$ ).

The gradient-descent update rule is  $\hat{w}_a(t+1) = \hat{w}_a(t) + \Delta\hat{w}_a(t)$ , where  $\Delta\hat{w}_a(t) = l_a \left[ -\frac{\partial E_a(t)}{\partial \hat{w}_a(t)} \right]$ ,  $l_a > 0$ .

The weights between the input layer and the hidden layer is updated by

$$\hat{w}_a^{(1)}(t+1) = \hat{w}_a^{(1)}(t) + \Delta\hat{w}_a^{(1)}(t) \quad (29)$$

where  $\hat{w}_c^{(1)} \in \mathbb{R}^{N_{h_c} \times m}$ , and the element-wise increment:

$$\Delta\hat{w}_{a,ji}^{(1)}(t) = l_a \left[ -\frac{\partial E_a(t)}{\partial \hat{w}_{a,ji}^{(1)}(t)} \right], \quad (30)$$

Applying the chain rule:

$$\begin{aligned} \frac{\partial E_a(t)}{\partial \hat{w}_{a,ji}^{(1)}(t)} &= \frac{\partial E_a(t)}{\partial e_a(t)} \left[ \frac{\partial e_a(t)}{\partial u(t)} \right]^T \frac{\partial u(t)}{\partial \phi_{a,j}(t)} \frac{\partial \phi_{a,j}(t)}{\partial \sigma_{a,j}(t)} \frac{\partial \sigma_{a,j}(t)}{\partial \hat{w}_{a,ji}^{(1)}(t)} \\ &= \frac{\partial E_a(t)}{\partial e_a(t)} \sum_{k=1}^n \frac{\partial e_a(t)}{\partial u_k(t)} \frac{\partial u_k(t)}{\partial \phi_{a,j}(t)} \frac{\partial \phi_{a,j}(t)}{\partial \sigma_{a,j}(t)} \frac{\partial \sigma_{a,j}(t)}{\partial \hat{w}_{a,ji}^{(1)}(t)} \\ &= \frac{\partial E_a(t)}{\partial e_a(t)} \left( \frac{\partial r(t)}{\partial u(t)} + \alpha \left[ \frac{\partial \hat{J}(t+1)}{\partial x(t+1)} \right]^T \frac{\partial x(t+1)}{\partial u(t)} \right)^T \frac{\partial u(t)}{\partial \phi_{a,j}(t)} \frac{\partial \phi_{a,j}(t)}{\partial \sigma_{a,j}(t)} \frac{\partial \sigma_{a,j}(t)}{\partial \hat{w}_{a,ji}^{(1)}(t)} \\ &= \frac{\partial E_a(t)}{\partial e_a(t)} \left( 2Ru(t) + \alpha \left[ \frac{\partial \hat{J}(t+1)}{\partial x(t+1)} \right]^T G(t-1) \right)^T \frac{\partial u(t)}{\partial \phi_{a,j}(t)} \frac{\partial \phi_{a,j}(t)}{\partial \sigma_{a,j}(t)} \frac{\partial \sigma_{a,j}(t)}{\partial \hat{w}_{a,ji}^{(1)}(t)} \\ &= e_a(t) \left( 2Ru(t) + \left[ \alpha \hat{w}_c^{(2)}(t) \phi'(x(t+1)) \hat{w}_c^{(1)}(t) \right]^T G(t-1) \right)^T \hat{w}_{a,j}^{(2)}(t) \phi'_{a,j}(x(t)) x_i(t) \end{aligned} \quad (31)$$

The weight between the hidden layer and the output layer is updated by

$$\hat{w}_a^{(2)}(t+1) = \hat{w}_a^{(2)}(t) + \Delta\hat{w}_a^{(2)}(t) \quad (32)$$

where  $\hat{w}_a^{(2)} \in \mathbb{R}^{n \times N_{h_a}}$ , and the element-wise increment:

$$\Delta\hat{w}_{a,kj}^{(2)}(t) = l_a \left[ -\frac{\partial E_a(t)}{\partial \hat{w}_{a,kj}^{(2)}(t)} \right] \quad (33)$$

Applying the chain rule:

$$\begin{aligned} \frac{\partial E_a(t)}{\partial \hat{w}_{a,kj}^{(2)}(t)} &= \frac{\partial E_a(t)}{\partial e_a(t)} \frac{\partial e_a(t)}{\partial u_k(t)} \frac{\partial u_k(t)}{\partial \hat{w}_{a,kj}^{(2)}(t)} \\ &= \frac{\partial E_a(t)}{\partial e_a(t)} \left( \frac{\partial r(t)}{\partial u(t)} + \alpha \left[ \frac{\partial \hat{J}(t+1)}{\partial x(t+1)} \right]^T \frac{\partial x(t+1)}{\partial u(t)} \right)_k \frac{\partial u_k(t)}{\partial \hat{w}_{a,kj}^{(2)}(t)} \\ &= e_a(t) \left( 2Ru(t) + \alpha \left[ \frac{\partial \hat{J}(t+1)}{\partial x(t+1)} \right]^T G(t-1) \right)_k \phi_{a,j}(t) \\ &= e_a(t) \left( 2Ru(t) + \left[ \alpha \hat{w}_c^{(2)}(t) \phi'(x(t+1)) \hat{w}_c^{(1)}(t) \right]^T G(t-1) \right)_k \phi_{a,j}(t) \end{aligned} \quad (34)$$

**Remark 2.** The essence of IHDP is abstracting the control effectiveness matrix of the dynamical system  $G(t-1)$  from a state-action function in Action Dependent Heuristic Dynamic Programming (ADHDP) framework, to improve the learning accuracy and efficiency. The matrix  $G$  is identified using Recursive Least Square (RLS) algorithm online.

## VII. CONVERGENCE ANALYSIS

### A. Basics of uniformly ultimately bounded stability

Denote the sub-optimal weights by  $w_c^*, w_a^*$ , defined as  $w_c^* = \arg \min_{\hat{w}_c} \left\| \hat{J}(t) - r(t) - \alpha \hat{J}(t+1) \right\|$ , and  $w_a^* = \arg \min_{\hat{w}_a} \left\| r(t) + \alpha \hat{J}(t) - \hat{w}_a \right\|$  if we assume that the desired ultimate objective  $U_c = 0$  corresponds to success. The estimation errors of the critic and actor weights are defined by  $\tilde{w}(t) := \hat{w}(t) - w^*$ . Then Equations 25, 28, 31,34 define a dynamical system of estimation errors for a nonlinear function  $F$ :

$$\tilde{w}(t+1) = \tilde{w}(t) - F(\hat{w}(t), \phi(t), \phi(t+1)) \quad (35)$$

**Definition 1.** A dynamical system is said to be uniformly ultimately bounded (UUB) with ultimate bound  $b > 0$ , if for any  $a > 0$  and  $t_0 > 0$ , there exists a positive number  $N = N(a, b)$  independent of  $t_0$ , such that  $\|\tilde{w}(t)\| \leq b$ , for all  $t \geq N + t_0$ , whenever  $\|\tilde{w}(t_0)\| \leq a$ .

**Theorem 1** (UUB of a discrete dynamical system). If, for system (35), there exists a function  $L(\tilde{w}(t), t)$  such that for all  $\tilde{w}(t_0)$  in a compact set  $K$ ,  $L(\tilde{w}(t), t)$  is positive definite and the first difference satisfies  $\Delta L(\tilde{w}(t), t) < 0$ , for  $\|\tilde{w}(t_0)\| > b$ , for some  $b > 0$  such that the  $b$ -neighborhood of  $\tilde{w}(t)$  is contained in  $K$ , then the system is UUB and the norm of the state is bounded within a neighborhood of  $b$ .

### B. Network weights increments

This subsection analyzes the convergence of critic and actor weights updated using gradient descent algorithm.

**Assumption 1.** The sub-optimal weights of the critic and actor are bounded as  $\|w_c^*\| \leq w_c^{\max}$ ,  $\|w_a^*\| \leq w_a^{\max}$ .

**Lemma 1.** Under Assumption 1, the first difference of  $L_1(t) = \frac{1}{l_c} \text{tr} \left[ (\tilde{w}_c^{(2)}(t))^T \tilde{w}_c^{(2)}(t) \right]$  is

$$\begin{aligned} \Delta L_1(t) &= \frac{1}{l_c} \left( \text{tr} [(\tilde{w}_c^{(2)}(t+1))^T \tilde{w}_c^{(2)}(t+1)] - \text{tr} [(\tilde{w}_c^{(2)}(t))^T \tilde{w}_c^{(2)}(t)] \right) \\ &= l_c e_c^2(t) \|\phi_c(t)\|^2 + \|e_c(t) - \tilde{w}_c^{(2)}(t) \phi_c(t)\|^2 - \|\zeta_c(t)\|^2 - e_c^2(t) \end{aligned} \quad (36)$$

where  $\zeta_c(t) = \tilde{w}_c^{(2)}(t) \phi_c(t)$  is the approximation error of the critic output.

*Proof.* Using the update law (34) and the fact that  $w_c^{*(2)}$  is time-invariant:

$$\tilde{w}_c^{(2)}(t+1) = \hat{w}_c^{(2)}(t+1) - w_c^{*(2)} = \tilde{w}_c^{(2)}(t) - l_c e_c(t) \phi_c^T(t) \quad (37)$$

where  $e_c(t)$  is a scalar.

Then

$$\begin{aligned} \left( \tilde{w}_c^{(2)}(t+1) \right)^T \tilde{w}_c^{(2)}(t+1) &= \left( \tilde{w}_c^{(2)}(t) - l_c e_c(t) \phi_c^T(t) \right)^T \left( \tilde{w}_c^{(2)}(t) - l_c e_c(t) \phi_c^T(t) \right) \\ &= \left( \hat{w}_c^{(2)}(t) \right)^T \tilde{w}_c^{(2)}(t) + l_c^2 e_c^2(t) \phi_c(t) \phi_c^T(t) \\ &\quad - l_c e_c(t) \left( \hat{w}_c^{(2)}(t) \right)^T \phi_c^T(t) - l_c e_c(t) \phi_c(t) \hat{w}_c^{(2)}(t) \end{aligned} \quad (38)$$

Taking the trace:

$$\text{tr} \left[ \left( \tilde{w}_c^{(2)}(t+1) \right)^T \tilde{w}_c^{(2)}(t+1) \right] = \text{tr} \left[ \left( \tilde{w}_c^{(2)}(t) \right)^T \tilde{w}_c^{(2)}(t) \right] + l_c^2 e_c^2(t) \|\phi_c(t)\|^2 - 2l_c e_c(t) \text{tr} \left( \phi_c(t) \tilde{w}_c^{(2)}(t) \right) \quad (39)$$

$$= \text{tr} \left[ \left( \hat{w}_c^{(2)}(t) \right)^T \tilde{w}_c^{(2)}(t) \right] + l_c^2 e_c^2(t) \|\phi_c(t)\|^2 - 2l_c e_c(t) \tilde{w}_c^{(2)}(t) \phi_c(t) \quad (40)$$

Since  $\tilde{w}_c^{(2)}(t) \phi_c(t)$  is a scalar, the cross term becomes

$$-2l_c e_c(t) \tilde{w}_c^{(2)}(t) \phi_c(t) = l_c \left( \|e_c(t) - \tilde{w}_c^{(2)}(t) \phi_c(t)\|^2 - \|\tilde{w}_c^{(2)}(t) \phi_c(t)\|^2 - e_c^2(t) \right) \quad (41)$$

Taking the difference:

$$\begin{aligned}
 \Delta L_1(t) &= L_1(t+1) - L_1(t) \\
 &= \frac{1}{l_c} \left( \text{tr}[(\tilde{w}_c^{(2)}(t+1))^T \tilde{w}_c^{(2)}(t+1)] - \text{tr}[(\tilde{w}_c^{(2)}(t))^T \tilde{w}_c^{(2)}(t)] \right) \\
 &= l_c e_c^2(t) \|\phi_c(t)\|^2 + \|e_c(t) - \tilde{w}_c^{(2)}(t) \phi_c(t)\|^2 - \|\tilde{w}_c^{(2)}(t) \phi_c(t)\|^2 - e_c^2(t)
 \end{aligned} \tag{42}$$

Define  $\zeta_c(t) = \tilde{w}_c^{(2)}(t) \phi_c(t)$ , one has

$$\Delta L_1(t) = \underbrace{l_c e_c^2(t) \|\phi_c(t)\|^2 + \|e_c(t) - \tilde{w}_c^{(2)}(t) \phi_c(t)\|^2 - \|\zeta_c(t)\|^2 - e_c^2(t)}_{\Delta L_1(t)} \tag{43}$$

□

**Lemma 2.** Under Assumption 1, the first difference of  $L_2(t) = \frac{1}{l_a \gamma_1} \text{tr}[(\tilde{w}_a^{(2)}(t))^T \tilde{w}_a^{(2)}(t)]$  is bounded by

$$\Delta L_2(t) \leq \frac{1}{\gamma_1} \left( - \left( 1 - l_a \|\phi_a(t)\|^2 \|C(t)\|^2 \right) e_a^2 + 4 \|r(t)\|^2 + 8\alpha^2 \|\zeta_c(t+1)\|^2 + 8\alpha^2 \|w_c^{*(2)} \phi_c(t+1)\|^2 + \|\zeta_a(t) C(t)\|^2 \right) \tag{44}$$

where  $\zeta_a(t) = \tilde{w}_a^{(2)}(t) \phi_a(t)$ .

**Proof of Lemma 2.**

The actor weights from the hidden layer to the output layer are updated according to (34):

$$\begin{aligned}
 \tilde{w}_a^{(2)}(t+1) &= \hat{w}_a^{(2)}(t+1) - w_a^{*(2)} \\
 &= \hat{w}_a^{(2)}(t) - l_a e_a(t) \left( 2Ru(t) + \left[ \alpha \hat{w}_c^{(2)}(t) \phi'(x(t+1)) \hat{w}_c^{(1)}(t) \right]^T G(t-1) \right) \phi_a^T(t) \\
 &= \tilde{w}_a^{(2)}(t) - l_a e_a(t) C(t) \phi_a^T(t)
 \end{aligned} \tag{45}$$

where  $C_k(t) = \left( 2Ru(t) + \left[ \alpha \hat{w}_c^{(2)}(t) \phi'(x(t+1)) \hat{w}_c^{(1)}(t) \right]^T G(t-1) \right)_k$ ,  $\phi_a \in \mathbb{R}^{N_{ah} \times 1}$ .

**Remark 3.**  $C(t)$  is defined differently from [Ref] given the objective function to improve the policy, i.e.,  $r(t) + \hat{J}(t+1)$  in IHDP and  $\hat{J}(t)$  in ADHDP.

$$\tilde{w}_a^{(2)}(t+1) = \tilde{w}_a^{(2)}(t) - l_a e_a(t) C(t) \phi_a^T(t) \tag{46}$$

$$\begin{aligned}
 \left( \tilde{w}_a^{(2)}(t+1) \right)^T \tilde{w}_a^{(2)}(t+1) &= \left( \tilde{w}_a^{(2)}(t) - l_a e_a(t) C(t) \phi_a^T(t) \right)^T \left( \tilde{w}_a^{(2)}(t) - l_a e_a(t) C(t) \phi_a^T(t) \right) \\
 &= \left( \tilde{w}_a^{(2)}(t) \right)^T \tilde{w}_a^{(2)}(t) + l_a^2 e_a^2(t) \phi_a(t) C^T(t) C(t) \phi_a^T(t) \\
 &\quad - l_a e_a(t) \left( \tilde{w}_a^{(2)}(t) \right)^T C(t) \phi_a^T(t) - l_a e_a(t) \phi_a(t) C^T(t) \tilde{w}_a^{(2)}(t)
 \end{aligned} \tag{47}$$

The trace is

$$\begin{aligned}
 \text{tr} \left[ \left( \tilde{w}_a^{(2)}(t+1) \right)^T \tilde{w}_a^{(2)}(t+1) \right] &= \text{tr} \left[ \left( \tilde{w}_a^{(2)}(t) \right)^T \tilde{w}_a^{(2)}(t) \right] + l_a^2 e_a^2(t) \|C(t)\|^2 \|\phi_a(t)\|^2 \\
 &\quad - 2l_a e_a(t) \text{tr} \left( \phi_a(t) C^T(t) \tilde{w}_a^{(2)}(t) \right)
 \end{aligned} \tag{48}$$

Consider the cross term:

$$\begin{aligned}
 -2l_a e_a(t) \text{tr} \left( \phi_a(t) C^T(t) \tilde{w}_a^{(2)}(t) \right) &= -2l_a e_a(t) \text{tr} \left( \tilde{w}_a^{(2)}(t) \phi_a(t) C^T(t) \right) \\
 &= -2l_a e_a(t) \text{tr} \left( \zeta(t) C^T(t) \right) \\
 &\leq l_a \left( \|e_a(t) - \zeta_a(t) C(t)\|^2 - \|\zeta_a(t) C(t)\|^2 - e_a^2(t) \right)
 \end{aligned} \tag{49}$$

where  $\zeta_a(t) = \tilde{w}_a^{(2)}(t) \phi_a(t)$ .

Therefore, the first difference is

$$\begin{aligned}\Delta L_2(t) &= L_2(t+1) - L_2(t) \\ &= \frac{1}{l_a \gamma_1} \text{tr} \left( \tilde{w}_a^{(2)}(t+1)^T \tilde{w}_a^{(2)}(t+1) - \tilde{w}_a^{(2)}(t)^T \tilde{w}_a^{(2)}(t) \right)\end{aligned}\quad (50)$$

After substituting this expression, we obtain

$$\Delta L_2(t) = \frac{1}{\gamma_1} \left( l_a e_a^2(t) \|C(t)\|^2 \|\phi_a(t)\|^2 + \|e_a(t) - \zeta_a(t)C(t)\|^2 - \|\zeta_a(t)C(t)\|^2 - e_a^2(t) \right)\quad (51)$$

Notice that  $(a-b)^2 - b^2 \leq 2a^2 + b^2$ , one has

$$\begin{aligned}\|e_a(t) - \zeta_a(t)C(t)\|^2 - \|\zeta_a(t)C(t)\|^2 &\leq 2\|e_a(t)\|^2 + \|\zeta_a(t)C(t)\|^2 \\ &\leq 2\|r(t) + \alpha \hat{J}(t+1)\|^2 + \|\zeta_a(t)C(t)\|^2 \\ &\leq 2\left(\|r(t)\| + \alpha \|\hat{J}(t+1)\|\right)^2 + \|\zeta_a(t)C(t)\|^2 \\ &\leq 4\|r(t)\|^2 + 4\alpha^2 \|\hat{w}_c^{(2)}\phi_c(t+1)\|^2 + \|\zeta_a(t)C(t)\|^2 \\ &\leq 4\|r(t)\|^2 + 4\alpha^2 \left\|(\tilde{w}_c^{(2)} + w_c^{*(2)})\phi_c(t+1)\right\|^2 + \|\zeta_a(t)C(t)\|^2 \\ &\leq 4\|r(t)\|^2 + 8\alpha^2 \|\tilde{w}_c^{(2)}\phi_c(t+1)\|^2 + 8\alpha^2 \|w_c^{*(2)}\phi_c(t+1)\|^2 + \|\zeta_a(t)C(t)\|^2 \\ &\leq 4\|r(t)\|^2 + 8\alpha^2 \|\tilde{w}_c^{(2)}\phi_c(t+1)\|^2 + 8\alpha^2 \|w_c^{*(2)}\phi_c(t+1)\|^2 + \|\zeta_a(t)C(t)\|^2.\end{aligned}\quad (52)$$

Finally, we obtain the following bound:

$$\Delta L_2(t) \leq \frac{1}{\gamma_1} \underbrace{\left( -\left(1 - l_a \|\phi_a(t)\|^2 \|C(t)\|^2\right) e_a^2 + 4\|r(t)\|^2 + 8\alpha^2 \|\zeta_c(t+1)\|^2 + 8\alpha^2 \|w_c^{*(2)}\phi_c(t+1)\|^2 + \|\zeta_a(t)C(t)\|^2 \right)}_{\Delta L_2(t)}\quad (53)$$

**Remark 4.** Note that  $\Delta L_2$  depends on  $C(t)$ , which incorporates the control-effectiveness matrix  $G_{t-1}$ . Thus, a system with high control effectiveness, i.e. a more “sensitive” system, may exhibit a larger bound. Intuitively, this matches our expectation.

**Remark 5.** If we introduce the normalization  $\|(\hat{w}_c^{(2)}(t))^T C(t)\|^2 = 1$  and fix the input-layer weights, then Lemmas 1–2 yield the results of Liu et al. (2012).

**Lemma 3.** Under Assumption 1, the first difference of  $L_3(t) = \frac{1}{l_c \gamma_2} \text{tr} \left[ (\tilde{w}_c^{(1)}(t))^T \tilde{w}_c^{(1)}(t) \right]$  is bounded by

$$\Delta L_3(t) \leq \frac{1}{\gamma_2} \left( l_c e_c^2(t) \|a(t)\|^2 \|y(t)\|^2 + \text{tr} \left[ y^T(t) a^T(t) \tilde{w}_c^{(1)}(t) \right]^2 + e_c^2(t) \right)\quad (54)$$

where  $\gamma_2 > 0$  is a weighting factor and  $a(t)$  is a vector with  $a_j(t) = \hat{w}_{c,j}^{(2)}(t) \phi_j'(t)$ ,  $j = 1, \dots, N_{hc}$ .

**Proof of Lemma 3.** Consider the update rule (25) of critic weights between input layer and hidden layer

$$\hat{w}_c^{(1)}(t+1) = \hat{w}_c^{(1)}(t) - l_c e_c(t) B(t)\quad (55)$$

where  $B_{ji}(t) = \hat{w}_{c,j}^{(2)}(t) \phi_j'(t) y_i(t)$ ,  $(i = 1, \dots, m, j = 1, \dots, N_{hc})$ .

The weight errors are

$$\tilde{w}_c^{(1)}(t+1) = \hat{w}_c^{(1)}(t+1) - w_c^{*(1)} = \tilde{w}_c^{(1)}(t) - l_c e_c(t) B(t)\quad (56)$$

$$\begin{aligned}\tilde{w}_c^{(1)}(t+1)^T \tilde{w}_c^{(1)}(t+1) &= \left( \tilde{w}_c^{(1)}(t) - l_c e_c(t) B(t) \right)^T \left( \tilde{w}_c^{(1)}(t) - l_c e_c(t) B(t) \right) \\ &= \left( \tilde{w}_c^{(1)}(t) \right)^T \tilde{w}_c^{(1)}(t) + l_c^2 e_c^2(t) B^T(t) B(t) \\ &\quad - l_c e_c(t) \left( \tilde{w}_c^{(1)}(t) \right)^T B(t) - l_c e_c(t) B^T(t) \tilde{w}_c^{(1)}(t)\end{aligned}\quad (57)$$

Introduce  $\text{tr}[B^T(t)B(t)] = \text{tr}[y^T(t)a^T(t)a(t)y(t)] = \|a(t)\|^2\|y(t)\|^2$ , and use  $\text{tr}(A^TB) = \text{tr}(B^TA)$ , the trace of the product becomes

$$\begin{aligned} \text{tr}\left(\tilde{w}_c^{(1)}(t+1)^T\tilde{w}_c^{(1)}(t+1)\right) &= \text{tr}\left[\tilde{w}_c^{(1)}(t)^T\tilde{w}_c^{(1)}(t)\right] + l_c^2e_c^2(t)\|a(t)\|^2\|y(t)\|^2 \\ &\quad - 2l_ce_c(t)\text{tr}[B^T(t)\tilde{w}_c^{(1)}(t)] \end{aligned} \quad (58)$$

Using inequality  $-2ab \leq a^2 + b^2$ , the cross term of (58) becomes

$$-2l_ce_c(t)\text{tr}[B^T(t)\tilde{w}_c^{(1)}(t)] \leq l_c\left(\text{tr}[B^T(t)\tilde{w}_c^{(1)}(t)]^2 + e_c^2(t)\right)$$

Therefore, the first difference can be bounded by

$$\Delta L_3(t) \leq \underbrace{\frac{1}{\gamma_2}\left(l_ce_c^2(t)\|a(t)\|^2\|y(t)\|^2 + \text{tr}\left[y^T(t)a^T(t)\tilde{w}_c^{(1)}(t)\right]^2 + e_c^2(t)\right)}_{\Delta L_3(t)} \quad (59)$$

**Lemma 4.** Under Assumption 1, the first difference of  $L_4(t) = \frac{1}{l_a\gamma_3}\text{tr}\left[\tilde{w}_a^{(1)}(t)^T\tilde{w}_a^{(1)}(t)\right]$  is bounded by

$$\Delta L_4(t) \leq \frac{1}{\gamma_3}\left(l_ae_a^2(t)\|C(t)D^T(t)\|^2\|x(t)\|^2 + e_a^2(t) + \|C(t)D^T(t)\|^2\left\|\tilde{w}_a^{(1)}(t)x(t)\right\|^2\right) \quad (60)$$

where  $\gamma_3 > 0$  is a weighting factor, and  $D_{ij}(t) = \hat{w}_{aj}^{(2)}(t)\text{sech}^2(x(t))$ ,  $i = 1, \dots, N_h^a$ ,  $j = 1, \dots, n$

**Proof of Lemma.** Consider the actor weights from the input layer to the hidden layer updated in (31):

$$\begin{aligned} \hat{w}_a^{(1)}(t+1) &= \hat{w}_a(t) - l_ae_a(t)C^T(t)D(t)\tilde{w}_a^{(1)}(t)x(t) \\ &= e_a(t)\left(2Ru(t) + \left[\alpha\hat{w}_c^{(2)}(t)\phi'(x(t+1))\hat{w}_c^{(1)}(t)\right]^T G(t-1)\right)^T \hat{w}_{a,j}^{(2)}(t)\phi'_{a,j}(x(t))x_i(t) \end{aligned} \quad (61)$$

The weight errors are

$$\begin{aligned} \tilde{w}_a^{(1)}(t+1) &= \hat{w}_a^{(1)}(t+1) - w_a^{*(1)} \\ &= \tilde{w}_a^{(1)}(t) - l_ae_a(t)C^T(t)D(t)x(t). \end{aligned} \quad (62)$$

$$\begin{aligned} \left(\tilde{w}_a^{(1)}(t+1)\right)^T \tilde{w}_a^{(1)}(t+1) &= \left(\tilde{w}_a^{(1)}(t) - l_ae_a(t)C^T(t)D(t)x(t)\right)^T \left(\tilde{w}_a^{(1)}(t) - l_ae_a(t)C^T(t)D(t)x(t)\right) \\ &= \left(\tilde{w}_a^{(1)}(t)\right)^T \tilde{w}_a^{(1)}(t) + l_a^2e_a^2x^T(t)D^T(t)C(t)C^T(t)D(t)x(t) \\ &\quad - l_ae_a(t)\left(\tilde{w}_a^{(1)}(t)\right)^T C^T(t)D(t)x(t) - l_ae_a(t)x^T(t)D^T(t)C(t)\tilde{w}_a^{(1)}(t) \end{aligned} \quad (63)$$

Take the trace operation, and  $\text{tr}[x^T(t)D^T(t)C(t)C^T(t)D(t)x(t)] = \|C^T(t)D(t)\|^2\|x(t)\|^2$ :

$$\begin{aligned} \text{tr}\left[\left(\tilde{w}_a^{(1)}(t+1)\right)^T \tilde{w}_a^{(1)}(t+1)\right] &= \text{tr}\left[\left(\tilde{w}_a^{(1)}(t)\right)^T \tilde{w}_a^{(1)}(t)\right] + l_a^2e_a^2(t)\|C^T(t)D(t)\|^2\|x(t)\|^2 \\ &\quad - 2l_ae_a(t)\text{tr}\left[x^T(t)D^T(t)C(t)\tilde{w}_a^{(1)}(t)\right] \end{aligned} \quad (64)$$

$$\text{tr}\left[x^T(t)D^T(t)C(t)\tilde{w}_a^{(1)}(t)\right] = \text{tr}\left[D^T(t)C(t)\tilde{w}_a^{(1)}(t)x^T(t)\right] \quad (65)$$

Using  $\text{tr}(A^TB + B^TA) = 2\text{tr}(A^TB)$ ,  $\text{tr}(AB) = \text{tr}(BA)$ .

The cross term in (64) can be transformed into the form:

$$-2l_ae_a(t)\text{tr}\left[C(t)D^T(t)\tilde{w}_a^{(1)}(t)x(t)\right] \leq l_a\left(e_a^2(t) + \|C(t)D^T(t)\|^2\left\|\tilde{w}_a^{(1)}(t)x(t)\right\|^2\right). \quad (66)$$

Based on the last result, we can obtain the upper bound

$$\Delta L_4(t) \leq \underbrace{\frac{1}{\gamma_3}\left(l_ae_a^2(t)\|C(t)D^T(t)\|^2\|x(t)\|^2 + e_a^2(t) + \|C(t)D^T(t)\|^2\left\|\tilde{w}_a^{(1)}(t)x(t)\right\|^2\right)}_{\Delta L_4(t)} \quad (67)$$

### C. Convergence of the weights errors

We introduce the Lyapunov candidate

$$L(t) = L_1(t) + L_2(t) + L_3(t) + L_4(t) \quad (68)$$

**Theorem 2 (Main Theorem).** Let the weights of the critic and actor be updated by gradient descent algorithm, and assume that the reward signal is a bounded semidefinite function. Under Assumption 1, the estimation errors  $w_a^* - \hat{w}_a(t)$  and  $w_c^* - \hat{w}_c(t)$  are uniformly ultimately bounded (UUB) if

$$l_c < \min_t \frac{\gamma_2 - \alpha}{\alpha^2 \gamma_2} \left( \|\phi_c(t)\|^2 + \frac{1}{\gamma_2} \|a(t)\|^2 \|y(t)\|^2 \right) \quad (69)$$

$$l_a < \min_t \frac{\gamma_3 - \gamma_1}{\gamma_3 \|(\hat{w}_c^{(2)}(t))^T C(t)\|^2 \|\phi_a(t)\|^2 + \gamma_1 \|\hat{w}_c^{(2)}(t) C(t) D^T(t)\|^2 \|x(t)\|^2} \quad (70)$$

**Proof of Theorem 2.** Collect all terms of  $\Delta L(t)$  based on the results of Lemmas 1–4,  $\Delta L(t)$  is bounded by

$$\Delta L(t) \leq (\Delta L_1) = l_c \underbrace{\|\phi_c(t)\|^2}_{2} \underbrace{e_c^2(t)}_{2} + \|e_c(t) - \tilde{w}_c^{(2)}(t) \phi_c(t)\|^2 - \underbrace{\|\zeta_c(t)\|^2}_{1} - \underbrace{e_c^2(t)}_{2} \quad (71)$$

$$(\Delta L_2) + \frac{1}{\gamma_1} \left( \left( l_a \|\phi_a(t)\|^2 \|C(t)\|^2 \right) \underbrace{e_a^2(t)}_{3} - \underbrace{e_a^2(t)}_{3} + 4 \|r(t)\|^2 + 8\alpha^2 \underbrace{\|\zeta_c(t+1)\|^2}_{1} + 8\alpha^2 \left\| w_c^{*(2)} \phi_c(t+1) \right\|^2 + \|C(t) \zeta_a(t)\|^2 \right) \quad (72)$$

$$(\Delta L_3) + \frac{1}{\gamma_2} \left( l_c \|a(t)\|^2 \|y(t)\|^2 \underbrace{e_c^2(t)}_{2} + \|\tilde{w}_c^{(1)}(t) y(t) a^T(t)\|^2 + \underbrace{e_c^2(t)}_{2} \right) \quad (73)$$

$$(\Delta L_4) + \frac{1}{\gamma_3} \left( l_a \underbrace{e_a^2(t)}_{3} \|C(t) D^T(t)\|^2 \|x(t)\|^2 + \underbrace{e_a^2(t)}_{3} + \|C(t) D^T(t)\|^2 \left\| \tilde{w}_a^{(1)}(t) x(t) \right\|^2 \right) \quad (74)$$

which yields

$$\begin{aligned} \Delta L(t) \leq & - \left( \|\zeta_c(t)\|^2 - \frac{8\alpha^2}{\gamma_1} \|\zeta_c(t+1)\|^2 \right) - \left( 1 - l_c \|\phi_c(t)\|^2 - \frac{l_c}{\gamma_2} \|a(t)\|^2 \|y(t)\|^2 - \frac{1}{\gamma_2} \right) e_c^2(t) \\ & - \left( \frac{1}{\gamma_1} - \frac{l_a}{\gamma_1} \|C(t)\|^2 \|\phi_a(t)\|^2 - \frac{l_a}{\gamma_3} \|D(t) C^T(t)\|^2 \|x(t)\|^2 - \frac{1}{\gamma_3} \right) e_a^2(t) \\ & + 4 \|r(t)\|^2 + \frac{8\alpha^2}{\gamma_1} \|w_c^{*(2)} \phi_c(t+1)\|^2 + \frac{1}{\gamma_1} \|C(t)\|^2 \|\zeta_a(t)\|^2 + \|w_c^{*(2)}(t) \phi_c(t) - r(t) - \alpha \hat{w}_c^{(2)}(t) \phi_c(t+1)\|^2 \\ & + \frac{1}{\gamma_2} \|\tilde{w}_c^{(1)}(t) y(t)\|^2 \|a(t)\|^2 \\ & + \frac{1}{\gamma_3} \|C(t) D^T(t)\|^2 \|\tilde{w}_a^{(1)}(t) x(t)\|^2 \end{aligned} \quad (75)$$

To ensure the negativity of the first term:

$$\begin{aligned} \frac{\gamma_1}{8\alpha^2} & > \frac{\|\zeta_c(t+1)\|^2}{\|\zeta_c(t)\|^2} \\ & = \frac{\|\tilde{w}^{(2)}(t)\|^2 \left( \|\phi(x(t))\|^2 + \|L \Delta x(t)\|^2 \right)}{\|\tilde{w}^{(2)}(t)\|^2 \|\phi(x(t))\|^2} \\ & = \frac{\|\phi(x(t))\|^2 + \|L \Delta x(t)\|^2}{\|\phi(x(t))\|^2} \\ & = 1 + \frac{\|L \Delta x(t)\|^2}{\|\phi(x(t))\|^2} \end{aligned} \quad (76)$$

where  $\Delta x(t) = x(t+1) - x(t)$ . The term  $\frac{\|L \Delta x(t)\|^2}{\|\phi(x(t))\|^2}$  is the effect of the state transition from  $x(t), x(t+1)$  on input to hidden layer of the critic, which can be proved to be upper bounded if  $x(t), w_c^{(1)}(t)$  are upper bounded:

$$\begin{aligned}
 \frac{\|L\Delta x(t)\|^2}{\|\phi(x(t))\|^2} &\leq \frac{\|L\|^2\|\Delta x(t)\|^2}{\|\tanh(w_c^{(1)}(t)x(t))\|^2} \\
 &\leq \frac{\|w_c^{(1)}(t)x(t)\|^2\|\Delta x(t)\|^2}{\|\tanh(w_c^{(1)}(t)x(t))\|^2} \\
 &\leq \frac{\|\bar{w}_c^{(1)}(t)\bar{x}(t)\|^2\|\Delta\bar{x}(t)\|^2}{\|\tanh(\bar{w}_c^{(1)}(t)\bar{x}(t))\|^2} \\
 &=\delta
 \end{aligned} \tag{77}$$

given the monotonicity of  $y = \frac{|x|^2}{|\tanh(x)|^2}$ .  $\|\Delta\bar{x}(t)\|$  is the upper bound of  $\|\Delta x(t)\|$  and determined by the system dynamics and the length of discrete time step.

To ensure negativity of the second and third term:

$$1 - l_c\|\phi_c(t)\|^2 - \frac{l_c}{\gamma_2}\|a(t)\|^2\|y(t)\|^2 - \frac{1}{\gamma_2} > 0. \tag{38}$$

Therefore,

$$l_c < \min_t \frac{\gamma_2 - 1}{\gamma_2(\|\phi_c(t)\|^2 + \frac{1}{\gamma_2}\|a(t)\|^2\|y(t)\|^2)}. \tag{39}$$

In particular,  $\gamma_2 > 1$ .

Similarly, for the actor:

$$\frac{1}{\gamma_1} - \frac{l_a}{\gamma_1}\|C(t)\|^2\|\phi_a(t)\|^2 - \frac{l_a}{\gamma_3}\|D(t)C^\top(t)\|^2\|x(t)\|^2 - \frac{1}{\gamma_3} > 0, \tag{40}$$

Therefore,

$$l_a < \min_t \frac{\gamma_3 - \gamma_1}{\gamma_3\|C(t)\|^2\|\phi_a(t)\|^2 + \gamma_1\|C(t)D^\top(t)\|^2\|x(t)\|^2} \tag{78}$$

In particular,  $\gamma_3 > \gamma_1$ .

The fourth term can be bounded as

$$\|w_c^{*(2)}\phi_c(t) - r(t) - \alpha\hat{w}_c^{(2)}(t+1)\phi_c(t+1)\|^2 \leq 4\|w_c^{*(2)}\phi_c(t)\|^2 + 4r^2(t) + 2\alpha^2\|\hat{w}_c^{(2)}(t+1)\phi_c(t+1)\|^2 \tag{79}$$

Let  $\bar{C}, \bar{w}_{a1}, \bar{w}_{a2}, \bar{w}_{c1}, \bar{\phi}_a, \bar{y}, \bar{x}, \bar{a}, \bar{D}$  be upper bounds of  $C, w_{a1}, w_{a2}, w_{c1}, \phi_a, y, x, a, D$ , and let  $w_{c2} = \max\{w_c^{*(2)}, w_{c2}^{(M)}\}$ , where  $w_{c2}^{(M)}$  is the upper bound of  $\hat{w}_c^{(2)}(t)$ . Finally, we obtain the following bound:

$$\begin{aligned}
 &\frac{4}{\gamma_1}\|w_c^{*(2)}\phi_c(t)\|^2 + \frac{1}{\gamma_1}\|\hat{w}_c^{(2)}(t)C(t)\|^2\|\zeta_a(t)\|^2 + \|\alpha w_c^{*(2)}\phi_c(t) + r(t) - \hat{w}_c^{(2)}(t-1)\phi_c(t-1)\|^2 \\
 &\quad + \frac{\alpha}{\gamma_2}\|\tilde{w}_c^{(1)}(t)y(t)\|^2\|a(t)\|^2 + \frac{1}{\gamma_3}\|\hat{w}_c^{(2)}(t)C(t)D^\top(t)\|^2\|\tilde{w}_a^{(1)}(t)x(t)\|^2 \\
 &\leq \left(\frac{4}{\gamma_1} + 4\alpha^2 + 2\right)(w_{c2}\phi_c)^2 + 4\bar{r}^2 + \frac{1}{\gamma_1}(\bar{w}_{c2}\bar{C}\bar{w}_{a2}\bar{\phi}_a)^2 + \frac{\alpha}{\gamma_2}(\bar{w}_{c1}\bar{y}\bar{a})^2 + \frac{1}{\gamma_3}(\bar{w}_{c2}\bar{C}\bar{D}\bar{w}_{a1}\bar{x})^2 = M.
 \end{aligned} \tag{43}$$

Therefore, if  $\gamma_1 > 8\alpha^2 \frac{\|\zeta(t+1)\|^2}{\|\zeta(t)\|^2}$  in the first term, and for  $l_a, l_c$  satisfying (39), (41), and  $\|\tilde{w}_c^{(2)}(t)\|^2 > \frac{M}{\|\phi(x(t))\|^2 - \frac{8\alpha^2}{\gamma_1}\|\phi(x(t+1))\|^2}$ , we obtain  $\Delta L(t) < 0$ . Based on Theorem 1, this implies that the system of estimation errors is ultimately uniformly bounded.

## VIII. APPLICATION ON FLIGHT CONTROL

### A. Critic

The critic neural network, with output  $\hat{J}$ , learns to approximate  $J$  function and its uses the output of the actor as one of its inputs. This is shown in Fig3.

### B. Outer-loop agent

The outer-loop agent aims to learn a sub-optimal policy for pitch rate reference required to track the angle-of-attack reference. The network structures are shown in Figure 2. The critic takes angle-of-attack, its tracking error and pitch rate as inputs. The output is the estimated state-value  $\hat{V}_1(t)$ . The absolute-value function  $\text{abs}(\cdot)$  is applied at the output layer to ensure positive definiteness. The actor uses control surface deflection as an additional input to attenuate the non-minimum phase dynamics. Its output is constrained using a scaled  $\tanh(\cdot)$  function to satisfy the limits on the pitch-rate reference.

1) *Critic*: The critic is updated through TD learning to minimize a loss function:

$$L_t^{C_1} = \frac{1}{2} \delta_{1(t)}^T \delta_{1(t)} \quad (80)$$

where  $\delta_{1(t)} = c_{1(t)} + \gamma \hat{V}'_{1(t+1)} - \hat{V}_{1(t)}$  is the TD error,  $\hat{V}'_1(\cdot)$  is a target critic used to delay weight updates and stabilize the learning process.

The gradient of  $L_t^{C_1}$  with respect to critic's parameter vector is

$$\hat{J}_t = \hat{w}_{c2,t}^T \sigma(w_{c1,t}^T e_t) \quad (81)$$

where  $w_{c1,t}$  and  $w_{c2,t}$  are weights of first and second layers,  $\sigma$  is the activation function. Let  $e_c(t) = \gamma \hat{J}_t + c_t - \hat{J}_{t-1}$  be the prediction error of the critic and  $E_{c,t} = \frac{1}{2} e_c^2$  be the objective function, which must be minimized. Let us consider gradient descent algorithm as the weight update rule, that is,  $\hat{w}_{c,t+1} = \hat{w}_{c,t} + \Delta \hat{w}_{c,t}$ . Here the last term is  $\Delta \hat{w}_{c,t} = l_c [-\frac{\partial E_{c,t}}{\partial \hat{w}_{c,t}}]$  and  $l_c > 0$  is the learning rate.

By applying the chain rule, the adaptation of the critic's weights between input layer and hidden layer is  $\Delta \hat{w}_{c,ij,t}^1 = l_c [-\frac{\partial E_{c,t}}{\partial \hat{w}_{c,ij,t}^1}]$ , which yields

$$\begin{aligned} \frac{\partial E_{c,t}}{\partial \hat{w}_{c,ij,t}^1} &= \frac{\partial E_{c,t}}{\partial \hat{J}_t} \frac{\partial \hat{J}_t}{\partial \phi_{ci,t}} \frac{\partial \phi_{ci,t}}{\partial \sigma_{c,i,t}} \frac{\sigma_{c,i,t}}{\partial \hat{w}_{c,ij,t}^1} \\ &= \gamma e_{c,t} \hat{w}_{ci,t}^{(2)} [\frac{1}{2} (1 - \phi_{ci,t}^2)] y_{j,t} \end{aligned} \quad (82)$$

The last calculation is obtained with respect to the main HDP paradigm, which treats  $\hat{J}(\cdot)$  at different time steps as different functions. Application of the chain rule for the adaptation of the critic between hidden and output layers yields  $\Delta \hat{w}_{c,i,t}^2 = l_c [-\frac{\partial E_{c,t}}{\partial \hat{w}_{c,i,t}^2}]$ , which leads to

$$\begin{aligned} \frac{\partial E_{c,t}}{\partial \hat{w}_{c,i,t}^2} &= \frac{\partial E_{c,t}}{\partial \hat{J}_t} \frac{\partial \hat{J}_t}{\partial w_{ci,t}^2} \\ &= \gamma e_{c,t} \phi_{ci,t} \end{aligned} \quad (83)$$

$$\frac{\partial L_t^{C_1}}{\partial w_t^{C_1}} = \frac{\partial L_t^{C_1}}{\partial \delta_{1(t)}} \frac{\partial \delta_{1(t)}}{\partial w_t^{C_1}} = -\delta_{1(t)} \frac{\partial \hat{V}_{1(t)}}{\partial w_t^{C_1}} \quad (84)$$

The critic is updated by stepping in opposite direction to the gradient of the loss with learning rate  $\eta_t^{C_1}$ :

$$w_t^{C_1} = w_t^{C_1} - \eta_t^{C_1} \frac{\partial L_t^{C_1}}{\partial w_t^{C_1}} \quad (85)$$

The target critic is updated by

$$w_{t+1}^{C_1'} = \tau w_t^{C_1} + (1 - \tau) w_t^{C_1'} \quad (86)$$

2) *Actor*: The training of the actor can be done by using the backpropagated adaptive critic method, which entails adapting the weights so as to  $\hat{J}_t$ . In this paper we used an importance-weighted training approach. We denote by  $U_c$  the desired ultimate objective function. Then the minimized error measure is given in the form  $E_{a,t} = \frac{1}{2} e_{a,t}^2$ , where  $e_{a,t} = \hat{J}_t - U_c$  is the prediction error of the actor:

$$\hat{u}(x_k) = \frac{1}{2} R^{-1} \hat{g}^T(x_k) \nabla \sigma_c^T(x_{k+1}) \hat{W}_{c,k} \quad (87)$$

where  $\nabla \sigma_c(x_{k+1}) = \frac{\partial \sigma_c}{\partial x_{k+1}}$ . To simplify expressions, we define  $\nabla \sigma_{c,k} = \nabla \sigma_c(x_k)$ ,  $\sigma_{a,k} = \sigma_a(x_k)$  and  $\epsilon_{a,k} = \epsilon_a(x_k)$ . The control input error is defined as

$$\tilde{u}(x_k) = \quad (88)$$

The actor is updated to minimize  $E_{a,t} = \frac{1}{2} e_{a,t}^2$ , where  $e_{a,t} = u_{t-1} - u_{t-1}^{\text{lar}}$ . The actor weights are updated with a learning rate  $l_a$ :

$$w_{a,t+1} = w_{a,t} - l_a \frac{\partial E_{a,t}}{\partial w_{a,t}} \quad (89)$$

3) *Training*: The forward propagation of action  $q_{\text{ref}}$  goes through the inner-loop actor to generate an action  $\delta$  that interacts with the model, seen as an additional control effectiveness. This implies that the outer-loop actor is equivalently interacting with an extended model that includes the inner-loop actor (see Figure 1). The training sample is given by  $(e_{1(t)}, \alpha_t, q_t, \delta_t, q_{\text{ref}}, e_{1(t+1)}, \alpha_{t+1}, q_{t+1})$ . Therefore, the gradient of the outer-loop actor propagates from  $\hat{V}'_{1(t+1)}$  and back through the inner-loop actor.

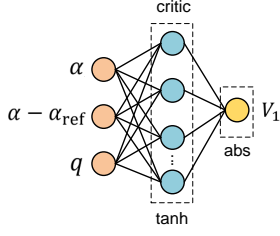


Fig. 2: Networks of outer-loop agent.

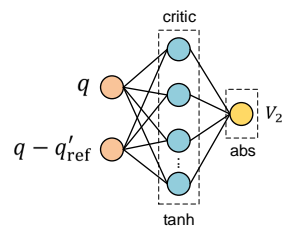
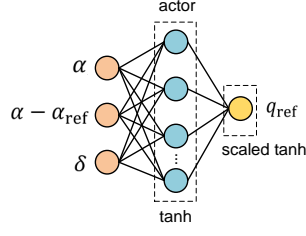
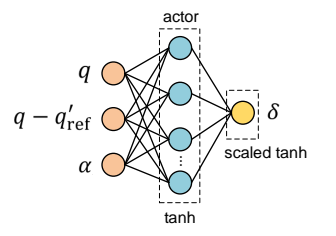


Fig. 3: Networks of inner-loop agent.



### C. Inner-loop agent

The inner-loop agent aims to learn a sub-optimal policy for control-surface deflection required to track the pitch-rate reference. The non-minimum-phase dynamics associated with  $\delta$  may unintentionally affect the  $\alpha$ -dynamics. This is a key motivation for adopting a cascaded control structure, which isolates this effect from the inner-loop agent's training process. As a result, the outer-loop agent is prevented from attempting to control angle-of-attack through the control-surface deflection directly.

Figure 3 shows the network structures as single-hidden-layer fully-connected multi-layer-perceptions (MLP). The inputs of the critic are the pitch rate and the its tracking error. The output is the estimated state-value  $\hat{V}_{2(t)}$ . An absolute-value function  $\text{abs}(\cdot)$  is applied at the output layer to ensure the positive definiteness. The actor uses angle-of-attack as an additional input to attenuate dynamic coupling in the  $q$ -dynamics. The output is the control surface deflection. A scaled  $\text{tanh}(\cdot)$  is applied at the output layer to constrain the action within actuator limits. The target critic and target actor share the same structures.

1) *Critic*: The critic is updated through Temporal Difference (TD) learning to minimize a loss function:

$$L_t^{C_2} = \frac{1}{2} \delta_{2(t)}^T \delta_{2(t)} \quad (90)$$

where  $\delta_{2(t)} = c_{2(t)} + \gamma \hat{V}'_{2(t+1)} - \hat{V}_{2(t)}$  is the TD error,  $\hat{V}'_2(\cdot)$  denotes the target critic, which is updated as a delayed version of  $\hat{V}_2(\cdot)$  to stabilize policy learning.

The gradient of the critic's loss with respect to its parameter vector is

$$\frac{\partial L_t^{C_2}}{\partial w_t^{C_2}} = \frac{\partial L_t^{C_2}}{\partial \delta_{2(t)}} \frac{\partial \delta_{2(t)}}{\partial w_t^{C_2}} = \delta_{2(t)} - \frac{\partial \hat{V}_{2(t)}}{\partial w_t^{C_2}} \quad (91)$$

The critic is updated by

$$w_{t+1}^{C_2} = w_t^{C_2} - \eta_t^{C_2} \frac{\partial L_t^{C_2}}{\partial w_t^{C_2}} \quad (92)$$

The target critic is updated by

$$w_{t+1}^{C'_2} = \tau w_t^{C_2} + (1 - \tau) w_t^{C'_2} \quad (93)$$

2) *Actor*: The actor is trained to minimize the estimated state-value function:

$$L_t^{A_2} = c_{2(t)} + \gamma \hat{V}'_{2(t+1)} \quad (94)$$

$$\delta_t^* = \arg \min_{\delta_t} L_t^{A_2} \quad (95)$$

The gradient of the actor's loss with respect to its parameter vector is

$$\begin{aligned} \frac{\partial L_t^{A_2}}{\partial w_t^{A_2}} &= \frac{\partial L_t^{A_2}}{\partial \delta_t} \frac{\partial \delta_t}{\partial w_t^{A_2}} \\ &= \left( 2b\delta_t + \frac{\partial \hat{V}'_2(e_{t+1}, q_{t+1}, \alpha_{t+1})}{\partial q_{t+1}} \frac{\partial q_{t+1}}{\partial \delta_t} \right) \frac{\partial \delta_t}{\partial w_t^{A_2}} \\ &= \left( 2b\delta_t + \frac{\partial \hat{V}'_2(e_{t+1}, q_{t+1}, \alpha_{t+1})}{\partial q_{t+1}} \hat{G}_{t-1} \right) \frac{\partial \delta_t}{\partial w_t^{A_2}} \end{aligned} \quad (96)$$

The actor is updated by

$$w_{t+1}^{A_2} = w_t^{A_2} - \eta_t^{A_2} \frac{\partial L_t^{A_2}}{\partial w_t^{A_2}} \quad (97)$$

3) *Training*: The training of the inner-loop actor is independent of the outer-loop actor, since the target critic  $\hat{V}'_{2(t+1)}$  propagates gradients only to the inner-loop actor. Therefore, the samples  $e_{1(t)}, e_{1(t+1)}$  are not used during training. The training sample is given by  $(e_{2(t)}, q_t, \alpha_t, \delta_t, e_{2(t+1)}, q_{t+1})$ . In this setting, the environment is treated as only the  $e_2$ -dynamics.

## IX. ACTION-SMOOTHING TECHNIQUES

This section introduces policy regularization for temporal smoothness technique and a low-pass filter to smoothen control actions. The first technique regularizes the actor to generate slow-varying actions, while the second technique filters the pitch rate reference.

### A. Policy regularization for temporal action smoothness

The temporal action smoothness measure the extent to which the output changes when the actor input changes:

$$L_{1(t)}^{\text{TS}} = |q_{\text{ref}(t+1)} - q_{\text{ref}(t)}| \quad (98)$$

$$L_{2(t)}^{\text{TS}} = |\delta_{t+1} - \delta_t| \quad (99)$$

where  $L_{1(t)}^{\text{TS}}, L_{2(t)}^{\text{TS}}$  are temporal smoothness (TS) losses for the outer-loop and inner-loop actors, respectively.

To reduce computation load in online learning, a single sample is used at each step of policy update to compute TS losses. This contrasts with using a minibatch in offline learning [29].

The multi-objective optimization frameworks are formulated as

$$q_{\text{ref}(t)}^* = \arg \min_{v_t} \left( c_{1(t)} + \gamma \hat{V}'_{1(t+1)} + \lambda_1 L_{1(t)}^{\text{TS}} \right) \quad (100)$$

$$\delta_t^* = \arg \min_{\delta_t} \left( c_{2(t)} + \gamma \hat{V}'_{2(t+1)} + \lambda_2 L_{2(t)}^{\text{TS}} \right) \quad (101)$$

where  $\lambda_1 \geq 0, \lambda_2 \geq 0$  are weights of TS losses.

### B. Low-pass filter

A second-order filter is used to smooth the pitch rate reference [30]:

$$\begin{aligned} \dot{d}_1 &= d_2 \\ \dot{d}_2 &= -2\zeta\omega_n^2 d_2 - \omega_n^2 (d_1 - q_{\text{ref}}) \end{aligned} \quad (102)$$

where  $d_1, d_2$  are filtered signal and its differentiation,  $\omega_n$  is the natural frequency,  $\zeta$  is the damping factor.

**Remark 6.** The training samples are collected under the Markov assumption for the environment, i.e., the one-step future state is determined solely by the current state. However, the states of the filter depend on the past two states due to its integral dynamics, which violates this assumption when a filter is used during the training of the outer-loop actor. As a result, the gradients from the value function  $\hat{V}_1$  are delayed by two time steps due to the filter. This issue can be mitigated by including the filter states as part of the environment state; however, this increases computational cost because of the higher dimensionality of the system and network inputs. To avoid delaying the gradient, this paper excludes the filter from the backpropagation of the policy through  $\hat{V}_1$  and applies it only during the forward propagation of the cascaded actor.

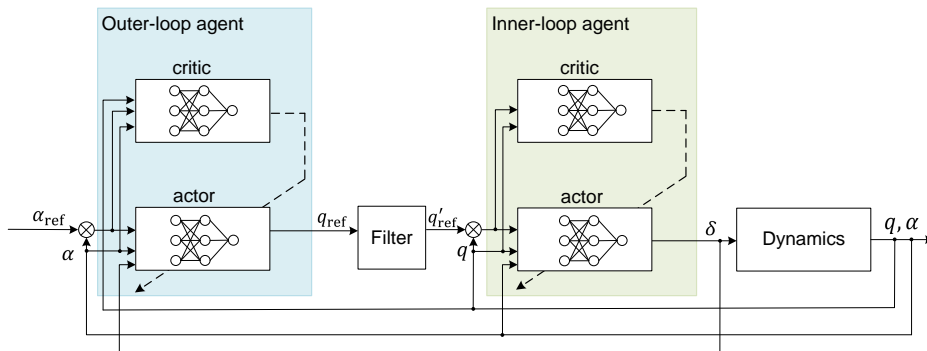


Fig. 4: Command-filtered cascaded online learning flight control system.

## X. SIMULATION

This section presents simulation results for cascaded online-learning flight control systems that incorporate action-smoothness conditioning techniques. The aerial vehicle dynamics are numerically simulated through the fourth-order Runge Kutta method. The actuator dynamics are modeled as a first-order system  $\tau \dot{\delta}_t + \delta_t = \delta_{c(t)}$ ,  $\tau = 0.005$ . To constrain actions, the outer-loop and inner-loop actors are scaled to  $[-20^\circ, 20^\circ]$  and  $[-20^\circ/\text{s}, 20^\circ/\text{s}]$ . The reference of angle-of-attack is set as  $\alpha_{\text{ref}(t)} = 10^\circ \sin(\frac{2\pi}{T}t)$ ,  $T = 10\text{s}$ . The network weights are randomly initialized using a uniform distribution  $\mathcal{U}(-0.01, 0.01)$ , which ensures an initially low-gain control law and slow learning to guard against inaccurate policy gradients. The persistence excitation signal is generated by adding Gaussian noise  $\mathcal{N}(0, 0.04)$  to the control surface deflection. The hyperparameters of the RL agents are listed in Table II. The baseline control system does not use either of action-smoothing techniques. We consider the tracking control performance in aspects of tracking errors, action smoothness, saturation level of activation function, actor sensitivity and one-step costs.

TABLE II: Hyperparameters of RL agents

Parameter	Outer-loop agent	Inner-loop agent
critic learning rate $\eta^{C1}, \eta^{C2}$	0.1	0.1
actor learning rate $\eta^{A1}, \eta^{A2}$	$5 \times 10^{-7}$	$10^{-7}$
discount factor $\gamma$	0.6	0.6
delay factor $\tau$	1	1
policy iteration number at each time step	3	3
hidden layer size	7	7
critic hidden-layer activation function	tanh	tanh
critic output layer activation function	abs	abs
actor activation function	tanh	tanh
optimizer	Adam	Adam
control effort weights $a, b$	$5 \times 10^{-6}$	$10^{-5}$
smoothness loss weight $\lambda_1, \lambda_2$	$9.3 \times 10^{-4}$	$10^{-5}$
loss thresholds for terminating critic training	$2.5 \times 10^{-4}$	$5 \times 10^{-5}$
maximal steps of critic and actor updates	50	50

### A. Temporal-smoothed control system

1) *Tracking control*: In Figure 5 the baseline control system exhibits satisfactory tracking performance during the first 10 seconds, but then experiences growing oscillations of the states and actions that degrade the convergence of the tracking error, ultimately leading to divergence. This issue is addressed in [Ref] by constraining the actions to the interval  $[-5^\circ, 5^\circ]$ , a hard constraint that does not prevent bang-bang control. In contrast, the temporal-smoothed control system produces smoother actions within  $[-6^\circ, 6^\circ]$  and avoids both divergence and bang-bang behavior by penalizing temporal variations in the actions. Figure 6 shows that the critic parameters of both the two systems converge to their sub-optimum within 10s, but the former continues to oscillate in response to large tracking errors. The actor parameters in the temporal-smoothed system exhibit slightly slower growth thanks to the stabilized tracking errors.

The frequency-domain characteristics of actions are captured by using the Fast Fourier Transform (FFT) algorithm, that converts the discrete-time action sequences into their frequency-domain representations, as given by the Discrete Fourier Transform  $X[k] = \sum_{n=0}^{N-1} x[n] e^{-j\frac{2\pi}{N}kn}$ ,  $k = 0, 1, \dots, N-1$ . Figures 7 and 8 show the time-domain histories and the spectra over the 0–100 Hz range. The signals of  $q_{\text{ref}}$  within 100 Hz are effectively attenuated using TS losses, and their amplitude of  $q_{\text{ref}}$  is significantly reduced without compromising tracking performance. Similar results are observed for control surface deflection. A reason for the oscillation of action  $\delta$  is that a switching tracking error  $e_2$  induced by the switching  $q_{\text{ref}}$  propagates through the lower-level actor to generate  $\delta$ .

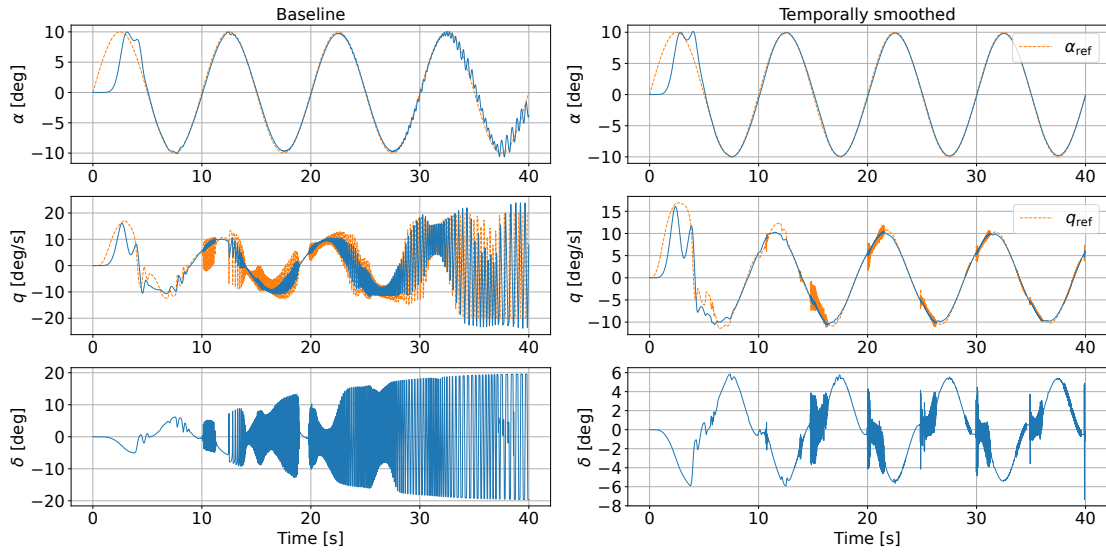


Fig. 5: Tracking control performance.

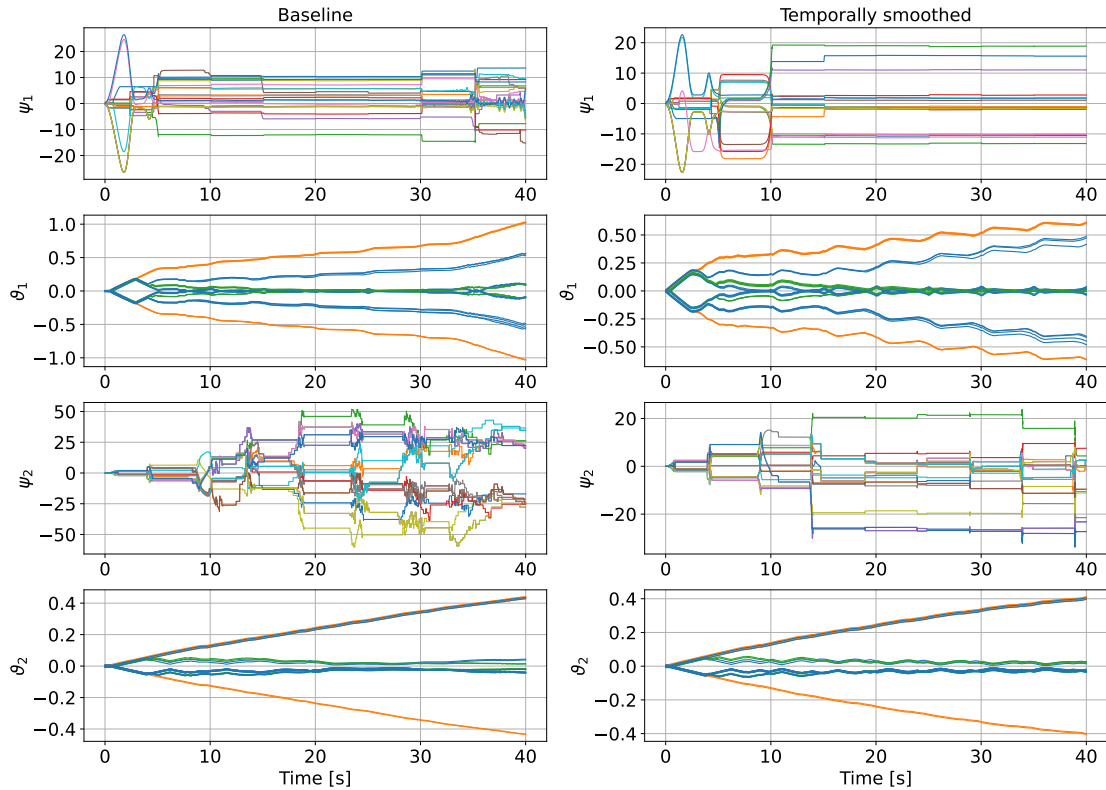


Fig. 6: Critic and actor parameters.

2) *Activation function*: The activation function  $\tanh(\cdot)$  is saturated if its output approaches the maximum or minimum value due to large inputs. In the saturated region of  $\tanh(\cdot)$ , its gradient vanishes and approaches zero (see Figure 9). The vanishing derivative leads to a vanishing policy gradient, resulting in slow learning of the control policy. Another effect is that the actor produces actions near their maximum or minimum limits in response to small tracking errors, resulting in an almost bang–bang control law that degrades tracking performance and system stability.

The saturation of the actor is the result of an aggressive process of policy learning. This occurs for two main reasons: (1) a large learning rate. A large learning rate causes the actor’s weights to be updated with large increments, pushing the activation function into its saturation zone, a process that is irreversible due to vanishing gradients. (2) Underemphasized control effort in the one-step cost function. An one-step cost function that underemphasizes the control effort does not discourage the actor to use large actions during learning. The vanishing gradients make these aggressive actions stay and persist to degrade the tracking

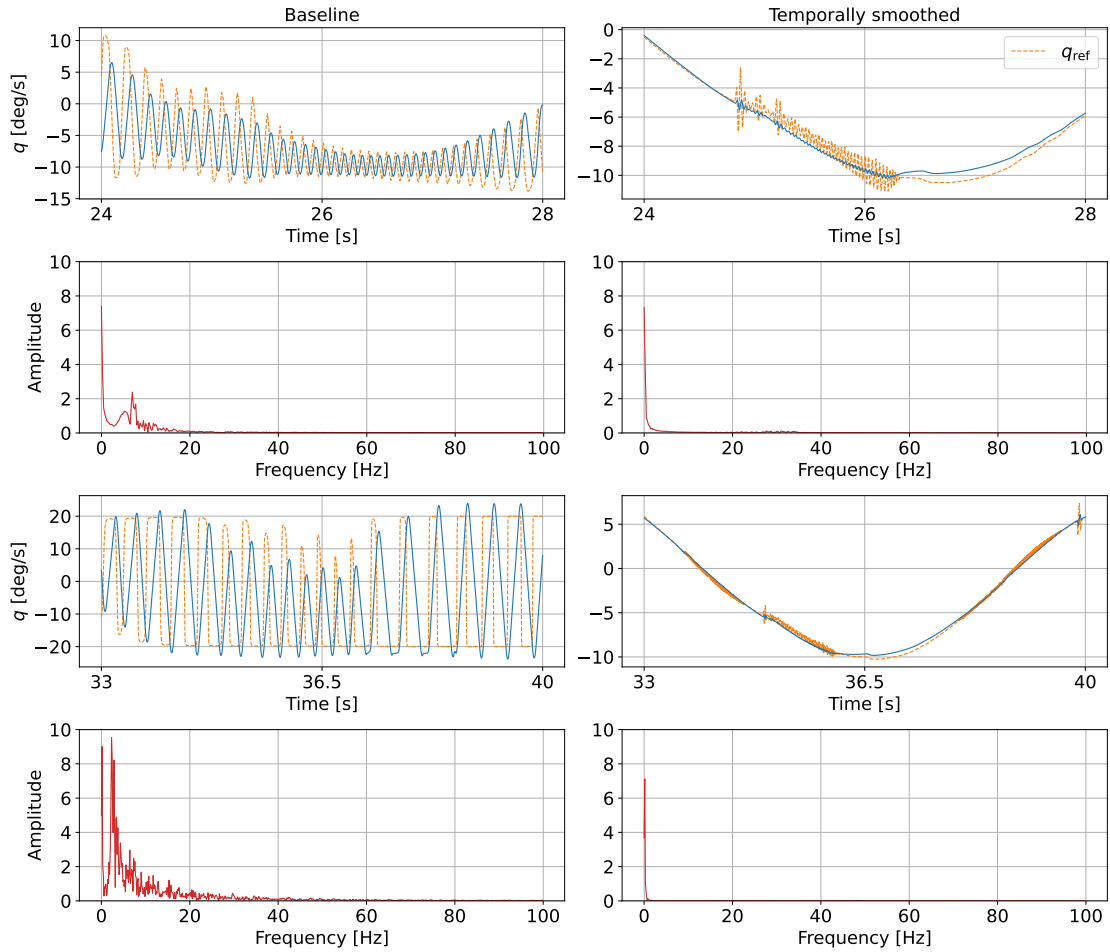


Fig. 7: Pitch rate in selected intervals.

performance even as the tracking error decreases. Between 10 and 20s, although  $\tanh(\cdot)$  is not saturated, significant switching actions occur, indicating that switching actions can happen even within the normal operating region of  $\tanh(\cdot)$ . Moreover, the time-varying dynamics and reference cause switching tracking errors, which propagate to the pitch-rate reference and control surface deflections through the cascaded actor.

Figure 9 shows the saturation level of  $\tanh(\cdot)$  in output layers of actors. The baseline control system eventually makes the inputs reach to intervals  $[-4,-2]$ ,  $[2,4]$  (the outer-loop actor) and intervals  $[-3,-2]$ ,  $[2,3]$  (the lower-level actor). In these intervals, the derivative is  $\tanh'(\cdot) \leq 0.1$  and attenuates the overall policy gradient. As a comparison, the temporal-smoothed control system avoids reaching to the saturation regions. The inputs are kept within 'unsaturated' interval  $[-2,2]$  (the outer-loop actor) and interval  $[-0.5,0.5]$  (the lower-level actor). This demonstrates the effectiveness of TS losses in avoiding saturation of  $\tanh(\cdot)$ .

3) *Action increment*: The one-step increment of pitch rate reference is

$$\Delta q_{\text{ref}(t+1)} = |q_{\text{ref}(t+1)} - q_{\text{ref}(t)}| \quad (103)$$

where  $q_{\text{ref}(t+1)} = W_1(e_1(t+1), \alpha_{t+1}, \delta_{t+1})$ ,  $q_{\text{ref}(t)} = W_1(e_1(t), \alpha_t, \delta_t)$  are actors' outputs.

The one-step increment of control surface deflection is

$$\Delta \delta_{t+1} = |\delta_{t+1} - \delta_t| \quad (104)$$

where  $\delta_{t+1} = W_2(e_2(t+1), q_{t+1}, \alpha_{t+1})$ ,  $\delta_t = W_2(e_2(t), q_t, \alpha_t)$  are actors' outputs .

Figure 10 shows the baseline control system suffers from fast-switching actions. Using a TS loss reduces the amplitude of the action increment to  $|\Delta q_{\text{ref}(t+1)}| \leq 0.5$  °s and decreases the amplitude of  $|\Delta \delta(t+1)|$ , resulting in less saturated control actions.

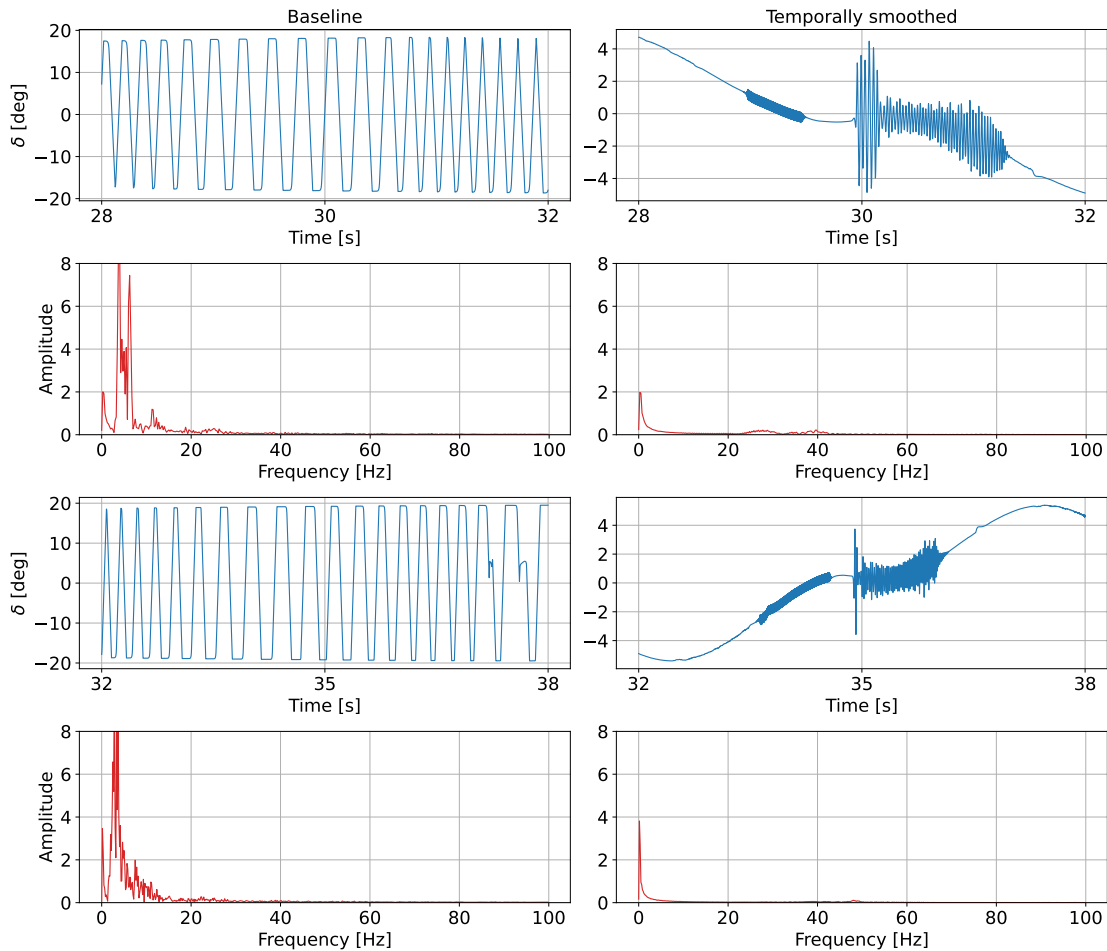


Fig. 8: Control surface deflection in selected intervals.

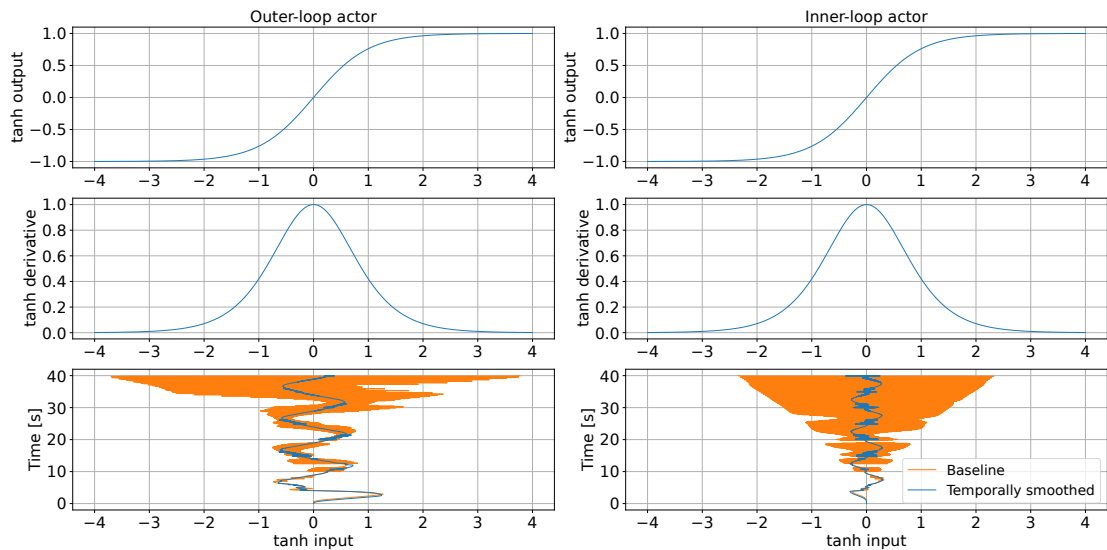


Fig. 9: Input of the activation function  $\tanh(\cdot)$  in output layers of actors.

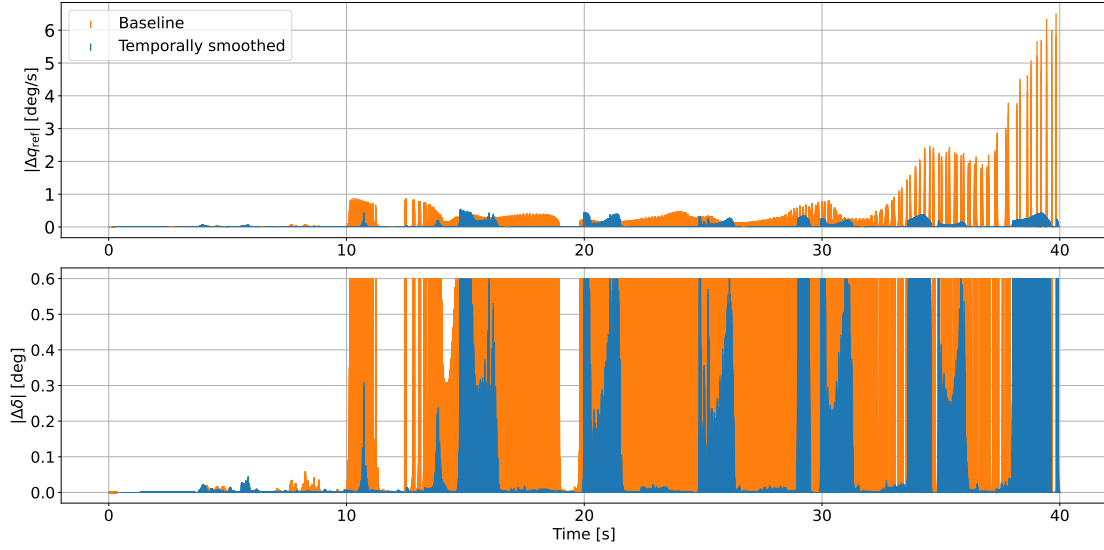


Fig. 10: Increments of actions.

4) *Actor sensitivity*: The sensitivity of the actor indicates how much, and in what direction, the output changes when the input increases slightly [34]. An actor with high sensitivity may overreact to its inputs, state variations and the tracking error. This is also correlated to robustness of the actor against sensor noise and uncertainties.

The sensitivity of the inner-loop and outer-loop actors is measured by

$$K_{1(t)} = \frac{\partial q_{\text{ref}(t)}}{\partial e_{1(t)}} \quad (105)$$

$$K_{2(t)} = \frac{\partial \delta(t)}{\partial e_{2(t)}} \quad (106)$$

The relation between the pitch rate reference and its sensitivity measure is

$$\begin{aligned} & |q_{\text{ref}(t+1)} - q_{\text{ref}(t)}| \\ & \approx |K_{1(t)}(e_{1(t+1)} - e_{1(t)})| \\ & = |K_{1(t)}| \cdot |e_{1(t+1)} - e_{1(t)}| \end{aligned} \quad (107)$$

Similarly, the relation between the control surface deflection and its sensitivity measure is

$$\begin{aligned} & |\delta_{(t+1)} - \delta_{(t)}| \\ & \approx |K_{2(t)}(e_{2(t+1)} - e_{2(t)})| \\ & = |K_{2(t)}| \cdot |e_{2(t+1)} - e_{2(t)}| \end{aligned} \quad (108)$$

Equations 107, 108 show that the action increments can be reduced through reducing sensitivity.

In Figure 11, the fast-growing  $K_1, K_2$  of the baseline control system indicate the actors are becoming significantly sensitive to variants of tracking errors. The oscillations are the results of actor saturation. The temporal-smoothed control system shows reduced oscillations because the TS losses penalize the increments of actions, which affects the actor sensitivity, as shown in Equations 107, 108.

5) *Challenges*: Although regularizing the policy using TS losses helps to generate smoother actions, the tuning of  $\lambda_1, \lambda_2$  remains empirical. Large values slow down the process of policy learning, while small values degrade action smoothness effect. Moreover, Figure 12 shows that the TS losses do not eliminate low-amplitude, high-frequency oscillations in  $\Delta q_{\text{ref}(t+1)}$  and  $\Delta \delta_{\text{ref}(t+1)}$ , since the penalization effects diminish when the increments are small (see Equations 98, 99). In this situation, a low-pass filter can be used, as it effectively removes high-frequency components from a frequency-domain perspective, thereby attenuating these action oscillations. Meanwhile, incorporating a low-pass filter into the flight control system does not interfere with the training process of actors.

### B. Command-filtered and temporal-smoothed control system

We introduce a low-pass filter into the cascaded online learning flight control system, which has been demonstrated effective in filtering pitch rate reference in backstepping [5]. The natural frequency and damping ratio are  $\omega_n = 20\text{rad/s}$  and  $\zeta = 0.7$ .

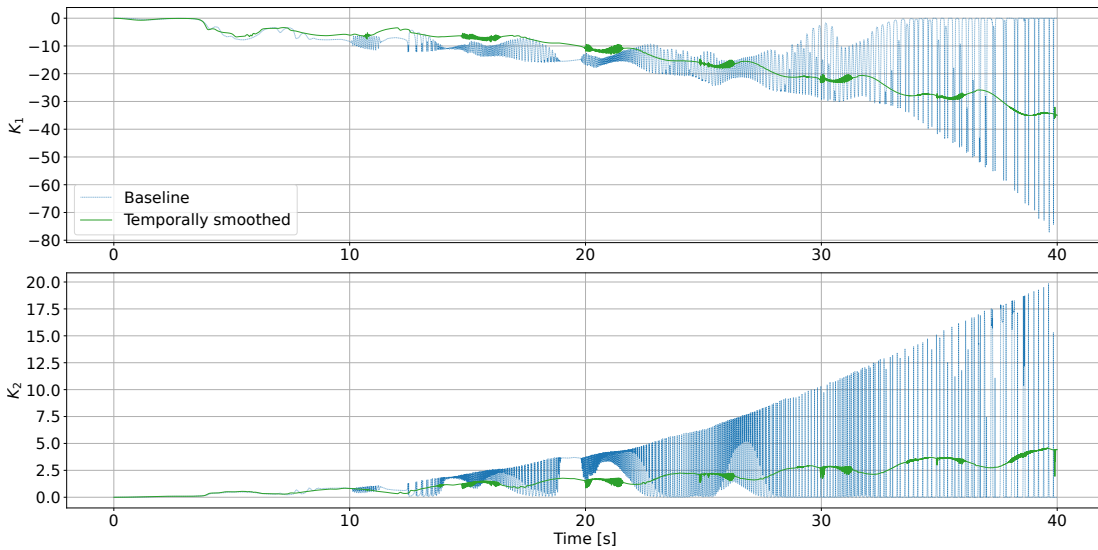


Fig. 11: Sensitivity measures.

1) *Tracking control:* Figure 12 compares the temporal-smoothed control system with its counterpart that includes a filter. The amplitude of the control surface deflection oscillation exceeds that of the pitch-rate reference oscillation, due to the proportional amplification of  $e_2$  by the inner-loop actor. The filter is capable of attenuating oscillations in pitch rate reference, leading to smooth  $e_2$  and smooth control surface deflection through the inner-loop actor. Figure 13 presents detailed comparisons of  $q_{ref}$  over selected time periods. The  $q_{ref}$  signals in the 10-40Hz range are effectively attenuated by the filter. Figure 14 provides detailed comparisons on  $\delta$  over selected time periods. The  $\delta$  signals in the 10-40Hz range are effectively attenuated. These observations account for the chosen filter parameters. Figure 15 shows the saturation level of  $\tanh(\cdot)$  in the output layer of actors. Both control systems prevent saturation of  $\tanh(\cdot)$ , ensuring that its derivative satisfies  $\tanh'(\cdot) \geq 0.4$  (the outer-loop actor) and  $\tanh'(\cdot) \geq 0.8$  (the inner-loop actor). The comparisons on  $K_1, K_2$  in Figure 16 show that applying a filter slows their growth and reduces oscillations, contributing to a more robust controller.

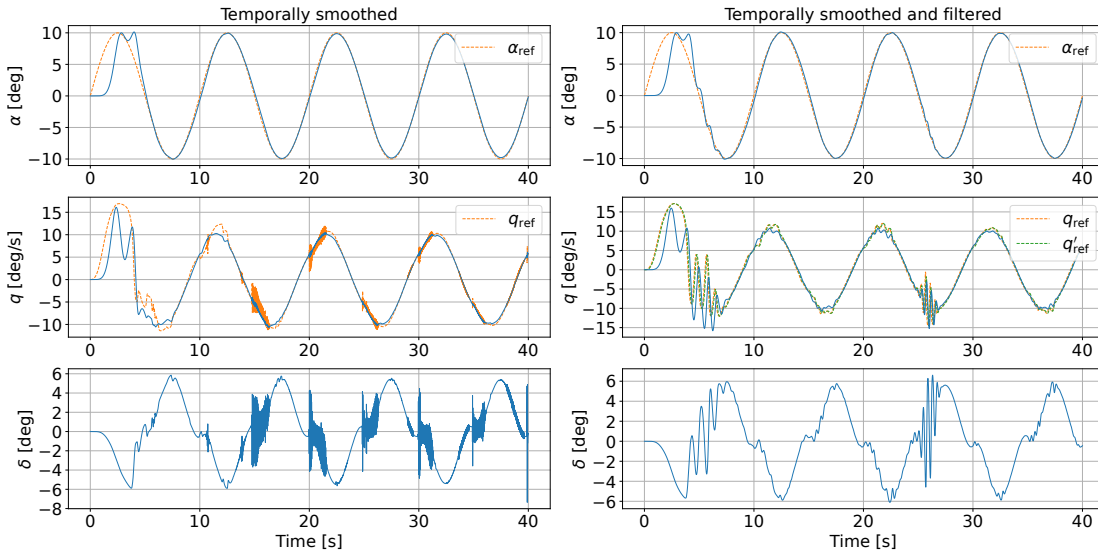


Fig. 12: Tracking performance comparison.

### C. Terminate and restart learning

1) *Termination:* The previous analysis assumes continual learning; that is, the agents never terminate learning during system operation. The issue lies in that growing control gains can cause state oscillations, even when tracking errors are small. Therefore, it is intuitive to terminate and restart learning based on tracking performance over a recent time period. Specifically, the actor is fixed if the accumulated tracking error over a period  $T_s$  remains within a specified threshold:

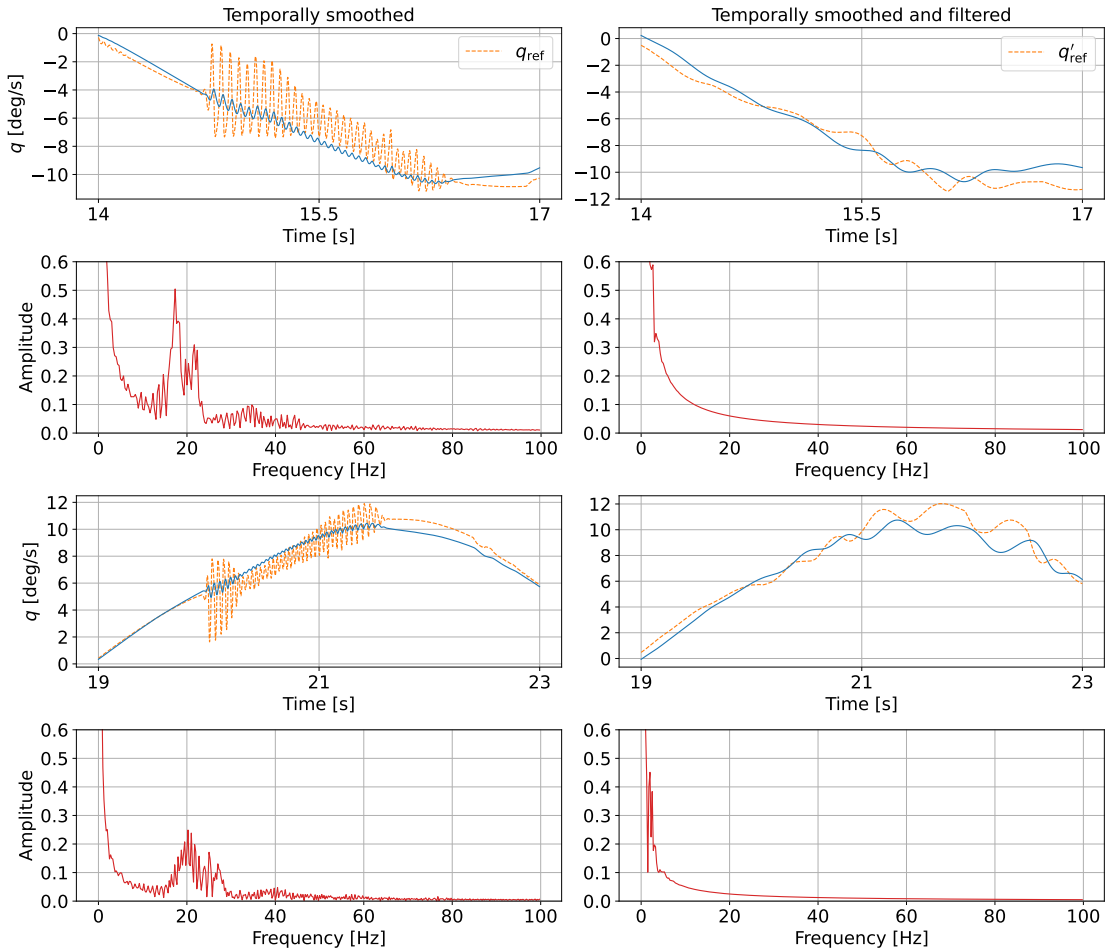


Fig. 13: Pitch rate in selected intervals.

$$\bar{e}_s \leq \epsilon \quad (109)$$

where  $\bar{e}_s = \frac{1}{n_s} \sum_{i=0}^{n_s-1} |e_{t-i}|$  is the average of absolute tracking errors,  $n_s = T_s/\Delta T$  is the number of samples,  $\epsilon > 0$  is an error threshold. A large error threshold makes learning terminated early when tracking errors are still large. Define the online-learning state indicator as  $\tau \in \{1, 0\}$ , with  $\tau = 1$  denoting that learning is off and  $\tau = 0$  denoting that learning is on.

During the initial phase, when  $t < T_s$  and there are not enough samples to compute  $\bar{e}_s$ , learning remains active:

$$\tau = 0, \text{ if } t < T_s \quad (110)$$

2) *Restart*: The learning must restart when the historical control performance degrades, typically occurring when the control system falls into faults and uncertainties. The restart condition determines in what case to restart learning. The evaluation period, denoted by  $T_r$ , should be carefully chosen to ensure it qualifies to represent the required control performance. A long evaluation period would delay the restart, preventing a timely response to performance degradation, while a short evaluation period makes the restart decision overly sensitive, potentially triggered by measurement noise or short-term peaks. As a result, the learning state may switch frequently between on and off.

The restart condition is

$$\bar{e}_r \geq \sigma \quad (111)$$

where  $\bar{e}_r = \frac{1}{n_r} \sum_{i=0}^{n_r-1} |e_{t-i}|$  is the average of absolute tracking errors,  $n_r = T_r/\Delta T$  is the number of samples,  $\sigma > 0$  is an error threshold. The sketch maps are provided in Figure 17. The pseudocode is seen in Algorithm 1.

The outer-loop and inner-loop agents have independent termination and restart conditions. Their parameters are seen in Table III. Figure 18 shows the histories of average tracking errors and the indicators. The outer-loop agent is turned off at 29s and restarted at 31.5s, while the inner-loop agent is turned off at 22s and is never restarted.

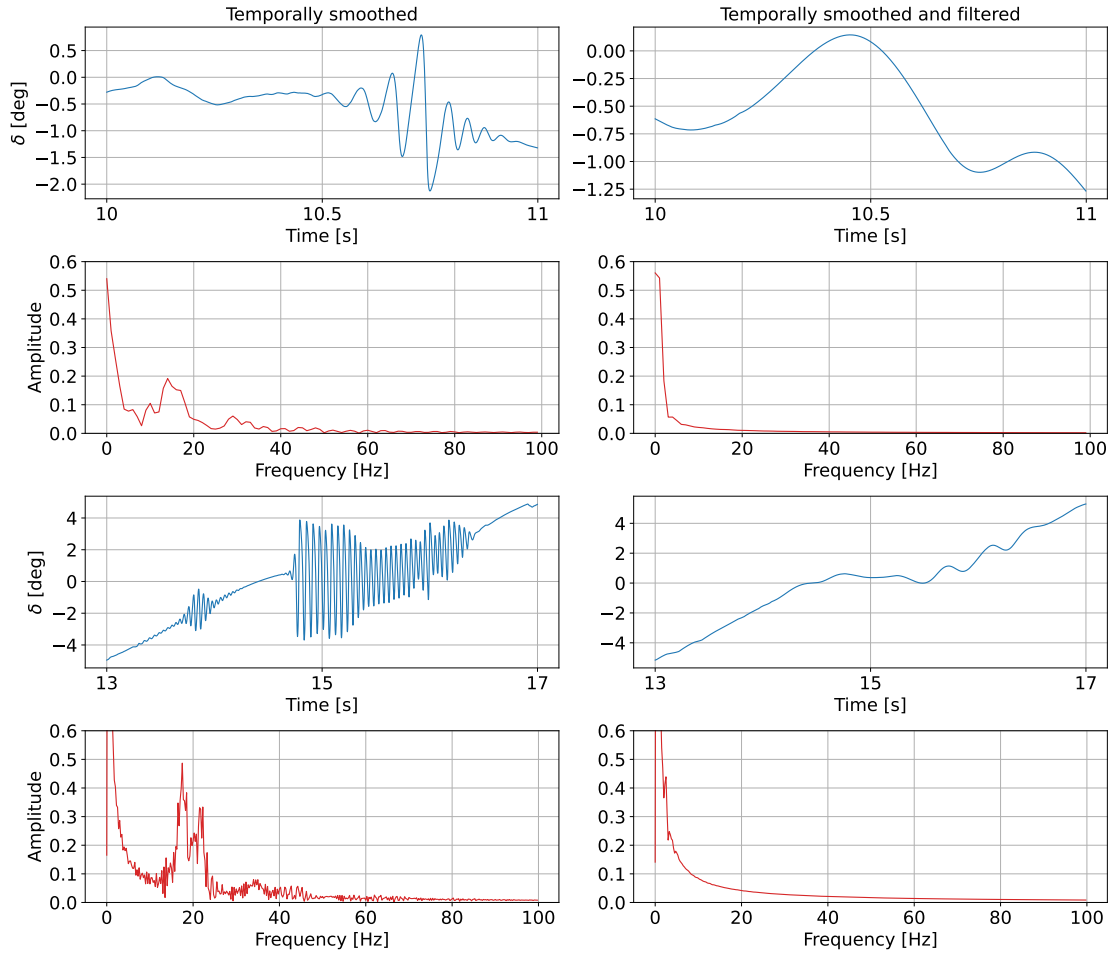


Fig. 14: Control surface deflection in selected intervals.

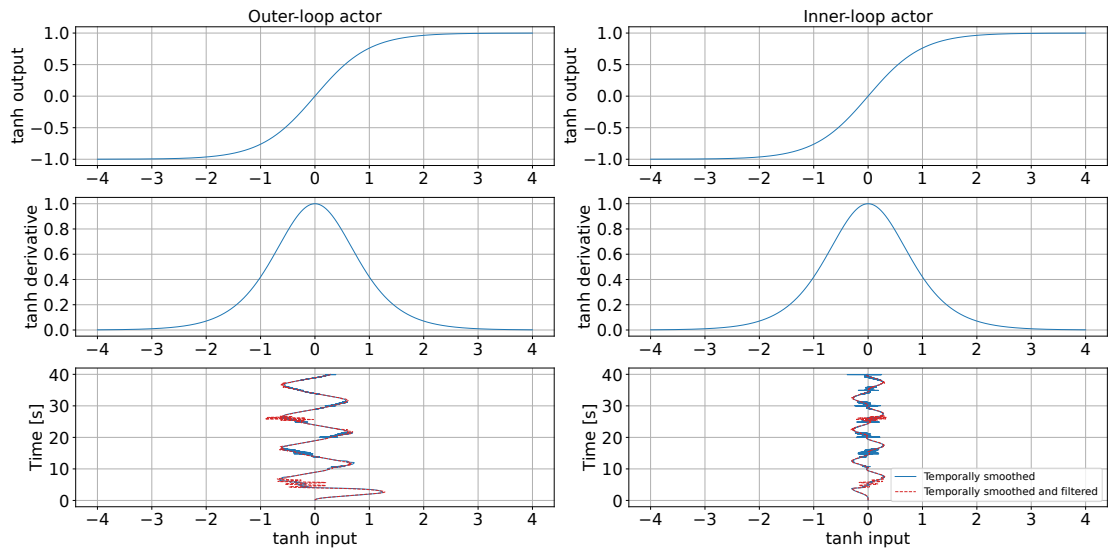


Fig. 15: Input of the activation function  $\tanh(\cdot)$  in the output layer of actors.

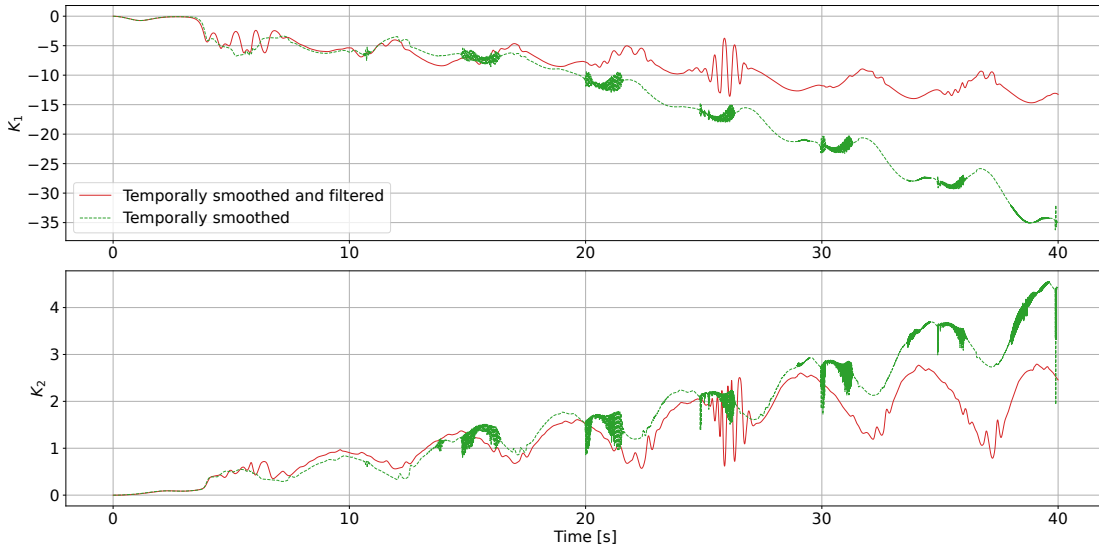


Fig. 16: Sensitivity measures.

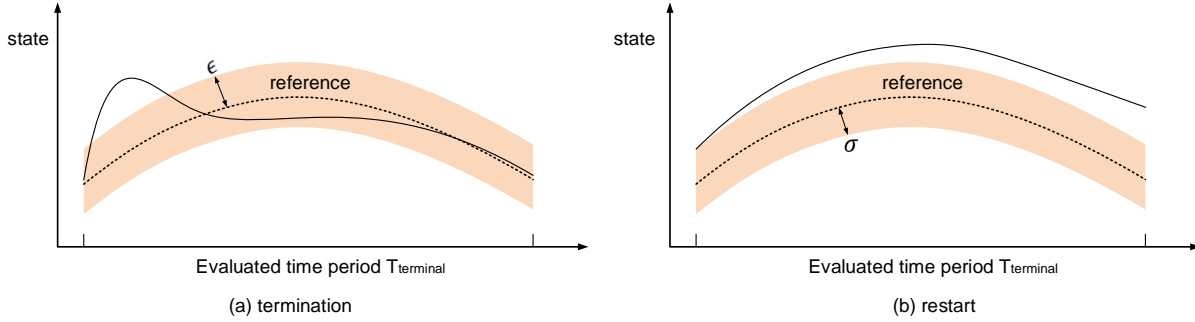


Fig. 17: Termination case (left) and restart case (right). The shaded area represents an average performance threshold. The actual average tracking errors must remain below this threshold to terminate learning, and exceed it to trigger a restart.

---

**Algorithm 1:** Termination and restart algorithm

---

**Data:**  $T_s, \epsilon, T_r, \sigma, t, \Delta T$

```

1 Initialization termination indicator  $\tau_{-1} = 0$ 
2 for each environment step  $t \leftarrow$  to  $t_{max}$  do
3   if  $\tau_{t-1} = 0$  then
4     if  $t \leq T_s$  then
5        $\tau_t = 0$ 
6     else
7       if  $\bar{e}_s \leq \epsilon$  then
8          $\tau_t = 1$ 
9       else
10         $\tau_t = 0$ 
11      end
12    end
13  end
14 end
15 if  $\tau_{t-1} = 1$  then
16   if  $\bar{e}_r \geq \sigma$  then
17      $\tau_t = 0$ 
18   else
19      $\tau_t = 1$ 
20   end
21 end

```

---

TABLE III: Parameters

Parameter	Outer-loop agent	Inner-loop agent
$T_s$	10s	10s
$\epsilon$	$0.25^\circ$	0.5deg/s
$T_r$	0.2s	0.1s
$\sigma$	$0.8^\circ$	2deg/s

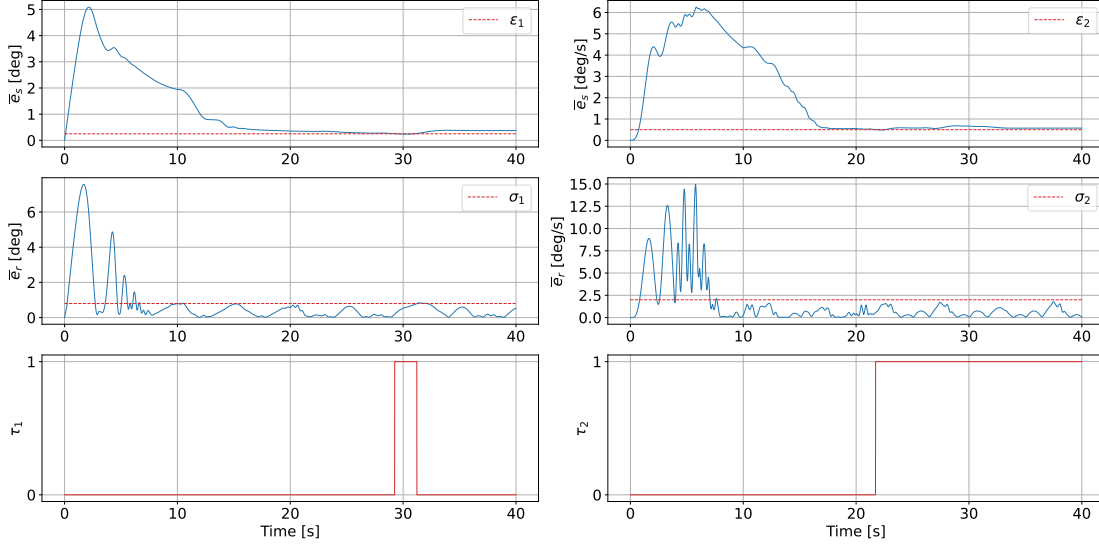


Fig. 18: Termination and restart measures.

## XI. CONCLUSION

We introduced two action-smoothing techniques into the cascaded online learning flight control system: temporal policy regularization and low-pass filter. The temporal policy regularization is verified through simulation to reduce the amplitude of pitch rate reference and control surface deflection. The low-pass filter is verified capable of removing the high-frequency signals of pitch rate reference, which cannot be accomplished by only using temporal policy regularization. The combination of these two methods enables a sufficient-level action smoothness during online learning. These techniques are necessary for online learning-based control of aerial vehicle systems with time-varying dynamics, suffering from oscillations of states and actions caused by switching tracking error.

## APPENDIX

## A. Derivation of incremental model

The continuous nonlinear system is given as

$$\dot{x}(t) = f(x(t), u(t)) \quad (112)$$

where the dynamics  $f: \mathbb{R}^n \times \mathbb{R}^m \rightarrow \mathbb{R}^n$  is a smooth function associated with state vector  $x \in \mathbb{R}^n$  and input vector  $u \in \mathbb{R}^m$ .  $n, m$  are positive integers denoting the dimensions of the state and action spaces.

Taking Taylor expansion for  $f(x(t), u(t))$  at  $t_0$ :

$$\begin{aligned} f(x(t), u(t)) &= f(x(t_0), u(t_0)) + F(t_0)(x(t) - x(t_0)) + G(t_0)(u(t) - u(t_0)) \\ &\quad + O[(x(t) - x(t_0))^2, (u(t) - u(t_0))^2] \end{aligned} \quad (113)$$

where  $F(t_0) = \partial f(x, u)/\partial x|_{x(t_0), u(t_0)} \in \mathbb{R}^{n \times n}$ ,  $G(t_0) = \partial f(x, u)/\partial u|_{x(t_0), u(t_0)} \in \mathbb{R}^{n \times m}$  are first-order partial derivatives at  $t_0$ .  $O(\cdot)$  is the summed higher-order terms.

The summed higher-order terms  $O(\cdot)$  have a relatively small effect on the change from  $x_t$  to  $x_{t+1}$  compared with the first-order terms. Moreover, these higher-order derivatives are difficult to identify from data, which poses challenges for practical application of an incremental model that includes them. For these two reasons, we omit  $O(\cdot)$  when defining an effective and practical model for the nonlinear system:

$$f(x(t), u(t)) = f(x(t_0), u(t_0)) + F(t_0)(x(t) - x(t_0)) + G(t_0)(u(t) - u(t_0)) \quad (114)$$

Using Equation 112:

$$\dot{x}(t) = \dot{x}(t_0) + F(t_0)[x(t) - x(t_0)] + G(t_0)[u(t) - u(t_0)] \quad (115)$$

The time derivatives are approximated by  $\dot{x}(t) \approx \frac{x(t+T) - x(t)}{T}$  and  $\dot{x}(t_0) \approx \frac{x(t_0+T) - x(t_0)}{T}$ , where  $T$  is a constant time step. Then

$$\frac{x(t+T) - x(t)}{T} \approx \frac{x(t_0+T) - x(t_0)}{T} + F(t_0)[x(t) - x(t_0)] + G(t_0)[u(t) - u(t_0)] \quad (116)$$

Define a discretization approach over  $T$  by setting  $t_0 = (k-1)T$ ,  $x(t_0) = x((k-1)T) \triangleq x_{k-1}$ . Let  $x(t)$  denote the next-step state following  $x(t_0)$ , then  $x(t) = x(t_0 + T) \triangleq x_k$ .

A discretized version of system 116 is

$$x_{k+1} - x_k \approx x_k - x_{k-1} + F_{k-1}(x_k - x_{k-1})T + G_{k-1}(u_k - u_{k-1})T \quad (117)$$

Use denotions  $\Delta x(k+1) = x(k+1) - x(k)$ ,  $\Delta x(k) = x(k) - x(k-1)$ ,  $\Delta u(k) = u(k) - u(k-1)$ :

$$\Delta x_{k+1} = \Delta x_k + F_{k-1}\Delta x_k T + G_{k-1}\Delta u_k T \quad (118)$$

## B. Recursive Least Squares identification

The linear forgetting Recursive Least Squares (RLS) algorithm is applied to identify matrices  $F_{t-1}, G_{t-1}$  are identified online. Define the augmented state as  $\mathbf{x}_t = [\Delta q_t, \Delta \delta_t]^T$  and estimated parameter vector as  $\hat{\theta}_{t-1} = [\hat{F}_{t-1}, \hat{G}_{t-1}]^T$ . The one-step state prediction is made as  $\Delta \hat{\mathbf{x}}_{t+1}^T = \mathbf{x}_t^T \hat{\theta}_{t-1}$ . The error between the true state and the predicted state is denoted by  $\varepsilon_t$  and defined as  $\varepsilon_t = \Delta \mathbf{x}_{t+1}^T - \Delta \hat{\mathbf{x}}_{t+1}^T$ . The parameter matrix is updated by

$$\hat{\theta}_t = \hat{\theta}_{t-1} + P_t \mathbf{x}_t \varepsilon_t \quad (119)$$

$$\begin{aligned} P_t^{-1} &= \alpha P_{t-1}^{-1} + \mathbf{x}_t \mathbf{x}_t^T \\ &= \sum_{j=1}^t \alpha^{t-j} \mathbf{x}_j \mathbf{x}_j^T + \alpha^t P_0^{-1} \\ &= \sum_{j=1}^t \alpha^{t-j} \mathbf{x}_j \mathbf{x}_j^T + I \alpha^t \lambda_{\min}(0) \end{aligned} \quad (120)$$

The initial auxiliary matrix is set as  $P_0 = I/\lambda_{\min}(0)$ , where  $0 < \lambda_{\min}(0) \ll 1$  is the minimum eigenvalue of  $P_0^{-1}$ . The initial parameter matrix is  $\hat{\theta}_0$ . The forgetting factor is  $0 \ll \alpha < 1$ .

## REFERENCES

- [1] J. D. Anderson *Fundamentals of Aerodynamics*. McGraw-Hill Series in Aeronautical and Aerospace Engineering. New York, USA: McGraw-Hill, 2017.
- [2] S. Sieberling, Q. P. Chu, and J. A. Mulder Robust Flight Control Using Incremental Nonlinear Dynamic Inversion and Angular Acceleration Prediction *Journal of Guidance, Control and Dynamics*, vol. 33, no. 6, pp. 1732–1742, 2010, doi: 10.2514/1.49978.
- [3] X. R. Wang, E. van Kampen, Q. P. Chu and P. Lu Stability Analysis for Incremental Nonlinear Dynamic Inversion Control *Journal of Guidance, Control and Dynamics*, vol. 42, no. 5, pp. 1116–1129, 2019, doi: 10.2514/1.G003791.
- [4] Z. C. Liu, Y. F. Zhang, and J. J. Liang and H. X. Chen Application of the Improved Incremental Nonlinear Dynamic Inversion in Fixed-Wing UAV Flight Tests *Journal of Aerospace Engineering*, vol. 35, no. 6, pp. 1–13, 2022, doi: 10.1061/(ASCE)AS.1943-5525.0001495.
- [5] Y. C. Wang, W. S. Chen, S. X. Zhang, J. W. Zhu and L. J. Cao Command-Filtered Incremental Backstepping Controller for Small Unmanned Aerial Vehicles *Journal of Guidance, Control, and Dynamics*, vol. 41, no. 4, pp. 952–965, 2018, doi: 10.2514/1.G003001.
- [6] X. R. Wang, E. van Kampen, Q. P. Chu and P. Lu Incremental Sliding-Mode Fault-Tolerant Flight Control *Journal of Guidance, Control, and Dynamics*, vol. 42, no. 2, pp. 244–259, 2019, doi: 10.2514/1.G003497.
- [7] W. H. Chen, J. Yang, L. Guo and S. H. Li Disturbance-Observer-Based Control and Related Methods—An Overview *IEEE Transactions on Industrial Electronics*, vol. 63, no. 2, pp. 1083–1095, 2016, doi: 10.1109/TIE.2015.2478397.
- [8] D. M. Acosta and S. S. Joshi Adaptive Nonlinear Dynamic Inversion Control of an Autonomous Airship for the Exploration of Titan *AIAA Guidance, Navigation and Control Conference and Exhibit*, Hilton Head, South Carolina, USA, August, 2007, doi: 10.2514/6.2007-6502.
- [9] E. J. J. Smeur, Q. P. Chu and G. H. E. de Croon Adaptive Incremental Nonlinear Dynamic Inversion for Attitude Control of Micro Air Vehicles *Journal of Guidance, Control, and Dynamics*, vol. 39, no. 3, pp. 450–461, 2016, doi: 10.2514/1.G001490.
- [10] B. Smit, T. S. C. Pollack and E. van Kampen Adaptive Incremental Nonlinear Dynamic Inversion Flight Control for Consistent Handling Qualities *AIAA SciTech 2022 Forum*, San Diego, CA&Virtual, USA, January, 2022, doi: 10.2514/6.2022-1394.
- [11] J. Harris, C. M. Elliott and G. S. Tallant L1 Adaptive Nonlinear Dynamic Inversion Control for the Innovative Control Effectors Aircraft *AIAA SciTech 2022 Forum*, San Diego, CA&Virtual, USA, January, 2022, doi: 10.2514/6.2022-0791.
- [12] L. Sonneveldt, Q. P. Chu and J. A. Mulder Constrained Adaptive Backstepping Flight Control: Application to a Nonlinear F-16/MATV Model *AIAA Guidance, Navigation and Control Conference and Exhibit*, Keystone, Colorado, USA, August, 2006, doi: 10.2514/6.2006-6413.
- [13] L. Sonneveldt, Q. P. Chu and J. A. Mulder Nonlinear Flight Control Design Using Constrained Adaptive Backstepping *Journal of Guidance, Control, and Dynamics*, vol. 30, no. 2, pp. 322–336, 2007, doi: 10.2514/1.25834.
- [14] Q. Hu, Y. Meng, C. L. Wang and Y. M. Zhang Adaptive Backstepping Control for Air-breathing Hypersonic Vehicles with Input Nonlinearities *Aerospace Science and Technology*, vol. 73, pp. 289–299, 2018, doi: 10.1016/j.ast.2017.12.001.
- [15] R. S. Sutton and A. G. Barto *Reinforcement Learning: An Introduction*. 6th edition, Sigma Series in Pure Mathematics. Cambridge, MA, USA: A Bradford Book, 2018.
- [16] Y. Zhou, E. van Kampen and Q.P. Chu Incremental Model Based Online Dual Heuristic Programming for Nonlinear Adaptive Control *Control Engineering Practice*, vol. 73, pp. 13–25, 2018, doi: 10.1016/j.conengprac.2017.12.011.
- [17] Y. Zhou, E. van Kampen and Q. P. Chu Incremental Approximate Dynamic Programming for Nonlinear Flight Control Design In *Proceedings of the EuroGNC 2015*, Toulouse, France, 2015.
- [18] Y. Zhou, E. van Kampen and Q. P. Chu Incremental Approximate Dynamic Programming for Nonlinear Adaptive Tracking Control with Partial Observability *Journal of Guidance, Control, and Dynamics*, vol. 41, no. 12, pp. 2554–2567, 2018, doi: 10.2514/1.G003472.
- [19] Y. Zhou, E. van Kampen and Q.P. Chu An Incremental Approximate Dynamic Programming Flight Controller Based on Output Feedback *AIAA Guidance, Navigation, and Control Conference*, San Diego, California, USA, January, 2016, doi: 10.2514/6.2016-0360.
- [20] B. Sun and E. van Kampen Incremental Model-Based Heuristic Dynamic Programming with Output Feedback Applied to Aerospace System Identification and Control *2020 IEEE Conference on Control Technology and Applications*, Montreal, QC, Canada, 2020, pp. 366-371, August, 2020, doi: 10.1109/CCTA41146.2020.9206261.
- [21] B. Sun and E. van Kampen Intelligent Adaptive Optimal Control Using Incremental Model-Based Global Dual Heuristic Programming Subject to Partial Observability *Applied Soft Computing*, vol. 103, pp. 1–15, 2021, doi: 10.1016/j.asoc.2021.107153.
- [22] B. Sun and E. van Kampen Reinforcement-Learning-Based Adaptive Optimal Flight Control with Output Feedback and Input Constraints *Journal of Guidance, Control, and Dynamics*, vol. 44, no. 9, pp. 1685–1691, 2021, doi: 10.2514/1.G005715.
- [23] B. Sun and E. van Kampen Event-Triggered Constrained Control Using Explainable Global Dual Heuristic Programming for Nonlinear Discrete-Time Systems *Neurocomputing*, vol. 468, pp. 452–463, 2022, doi: 10.1016/j.neucom.2021.10.046.
- [24] Y. Zhou, E. van Kampen and Q.P. Chu Incremental Model Based Heuristic Dynamic Programming for Nonlinear Adaptive Flight Control In *Proceedings of the International Micro Air Vehicles Conference and Competition*, Beijing, China, October, 2016, url: <https://www.imavs.org/papers/2016/25.pdf>.
- [25] Y. Zhou, E. van Kampen and Q. P. Chu Incremental Model based Online Heuristic Dynamic Programming for Nonlinear Adaptive Tracking Control with Partial Observability *Aerospace Science and Technology*, vol. 105, pp. 1–14, 2020, doi: 10.1016/j.ast.2020.106013.
- [26] S. Heyer, D. Kroezen and E. van Kampen Online Adaptive Incremental Reinforcement Learning Flight Control for a CS-25 Class Aircraft *AIAA Scitech 2020 Forum*, Orlando, FL, USA, October, 2020, doi: 10.2514/6.2020-1844.
- [27] L.G. Sun, C.C. de Visser, Q.P. Chu and W. Falkena Hybrid Sensor-Based Backstepping Control Approach with Its Application to Fault-Tolerant Flight Control *Journal of Guidance, Control, and Dynamics*, vol. 31, no. 1, pp. 59–71, 2014, doi: 10.2514/1.61890.
- [28] Y. Zhou, E. van Kampen and Q.P. Chu Launch Vehicle Adaptive Flight Control with Incremental Model Based Heuristic Dynamic Programming *International Astronautical Congress*, Adelaide, Australia, September, 2017.
- [29] S. Mysore, B. Mabsout, R. Mancuso and K. Saenko Regularizing Action Policies for Smooth Control with Reinforcement Learning *IEEE International Conference on Robotics and Automation*, Xi'an, China, October, 2021, doi: 10.1109/ICRA48506.2021.9561138.
- [30] A.N. Kalliny, A.A. El-Badawy and S.M. Elkhamsy Command-Filtered Integral Backstepping Control of Longitudinal Flapping-Wing Flight *Journal of Guidance, Control, and Dynamics*, vol. 41, no. 7, pp. 1556–1568, 2018, doi: 10.2514/1.G003267.
- [31] J.A. Farrell, M. Polycarpou, M. Sharma and W. Dong Command Filtered Backstepping *IEEE Transactions on Automatic Control*, vol. 54, no. 6, pp. 1391-1395, 2009, doi: 10.1109/TAC.2009.2015562.
- [32] R.A. Hull, D. Schumacher and Z.H. Qu Design and Evaluation of Robust Nonlinear Missile Autopilots from a Performance Perspective In *Proceedings of 1995 American Control Conference*, Seattle, WA, USA, June, 1995, doi: 10.1109/ACC.1995.529235.
- [33] P. J. Werbos Advanced Forecasting Methods for Global Crisis Warning and Models of Intelligence *General Systems*, vol. 22, pp. 25-38, 1977, url: <https://gwern.net/doc/reinforcement-learning/1977-werbos.pdf>.
- [34] K. Shibata Dynamic Reinforcement Learning for Actors *arXiv preprint*, 2025, doi: 10.48550/arXiv.2502.10200.
- [35] B. Sun and E. van Kampen Incremental Model-Based Global Dual Heuristic Programming with Explicit Analytical Calculations Applied to Flight Control *Engineering Applications of Artificial Intelligence*, vol. 89, pp. 103425, 2020, doi: 10.1016/j.engappai.2019.103425.